Plasticity, exudation and microbiome-association of the root system of Pellitory-of-the-wall plants grown in environments impaired in iron availability

Plasticity, exudation and microbiome-association of the root system of Pellitory-of-the-wall plants grown in environments impaired in iron availability

Liliana Tato[a], Vincenzo Lattanzio[b], Enrico Ercole[c], Marta Dell'Orto[a], Agostino Sorgonà[e], Vito Linsalata[d], Alessandra Salvioli di Fossalunga[c], Mara Novero[c], Stefania Astolfi[f], Maria Rosa Abenavoli[e], Irene Murgia[g], Graziano Zocchi[a], Gianpiero Vigani[c,]

[a] *Dipartimento di Scienze Agrarie e Ambientali, Produzioni, Territorio, Agroenergia, Universita` degli Studi di Milano, Italy*

[b] *Dipartimento di Scienze Agrarie, degli Alimenti e dell'Ambiente, Universita` degli Studi di Foggia, Italy*

[c] *Dipartimento di Scienze della Vita e Biologia dei Sistemi, Universita` degli Studi di Torino, Italy*

[d] *C.N.R. Istituto di Scienze delle Produzioni Alimentari, Bari, Italy*

[e] *Dipartimento Agraria, Universita` "Mediterranea" di Reggio Calabria Feo di Vito, 89124, Reggio Calabria, Italy*

[f] *DAFNE, Universita` della Tuscia, Viterbo, Italy*

[g] *Dipartimento di Bioscienze, Universita` degli Studi di Milano, Milano, Italy*

Keywords: Calcareous soil, Iron deficiency, Microbiome, *Parietaria Judaica*, Pellitory-of-the-wall, Phenols, Rhizosphere, Root architecture, Urban habitat

Abstract

The investigation of the adaptive strategies of wild plant species to extreme environments is a challenging issue, which favors the identification of new traits for plant resilience. We investigated different traits which characterize the root-soil interaction of *Parietaria judaica*, a wild plant species commonly known as "Pellitory-of-the- wall". *P. judaica* adopts the acidification-reduction strategy (Strategy I) for iron (Fe) acquisition from soil, and it can complete its life cycle in highly calcareous environments without any symptoms of chlorosis. In a field-to-lab approach, the microbiome associated with *P. judaica* roots was analyzed in spontaneous plants harvested from an urban environment consisting in an extremely calcareous habitat. Also, the phenolics and carboxylates content and root plasticity and exudation were analyzed in *P. judaica* plants grown under three different controlled conditions mimicking the effect of calcareous environments on Fe availability: results show that *P. judaica* differentially modulates root plasticity under different Fe

availability-impaired conditions, and that it induces, to a high extent, the exudation of caffeoylquinic acid derivatives under calcareous conditions, positively impacting Fe solubility.

Introduction

Variations in soil pH are among the abiotic factors affecting most plant growth, since they influence the bioavailability of essential nutrients and toxic elements for plants. The presence of carbonates in soils causes a decrease in the solubility of iron (Fe) and other micronutrients (Lindsay and Schwab, 1982; Schenkeveld and Kraemer, 2018). Calcareous soils, representing 30% of the Earth's land surface, are characterized by high pH values and may contain high HCO^- ions in the soil solution. Iron deficiency-induced chlorosis, otherwise known as lime chlorosis, is a major nutritional disorder observed in crops growing in calcareous soils; on one hand, alkaline pHs dramatically reduce Fe solubility in soil and on the other hand, the presence of HCO_3^- may interfere with the physiological processes of Fe uptake (Chen and Barak, 1982; Romheld, 1987; Kim and Guerinot, 2007; Díaz et al., 2012). Plant roots grown under calcareous conditions may exhibit a higher Fe content than those grown under non-calcareous conditions, indicating that low Fe availability in soil is not the unique factor causing lime-induced chlorosis; indeed, the composition of the soil itself can also influence Fe uptake from the apoplast (Mengel, 1994). Iron is an essential micronutrient for the energy-yielding electron transfer reactions of respiration and photosynthesis and other major metabolic processes in plants (Kobayashi and Nishizawa, 2012; Vigani and Murgia, 2018); the elucidation of plant adaptive growth strategies in calcareous habitats represents a valuable approach for the identification of tolerance traits under soil constraints. In this context, a characterization of *Arabidopsis thaliana* demes locally adapted in their native habitat to soils with high carbonate has recently been made (Ter´es et al., 2019).

The understanding of plant resilience to different biotic and abiotic stresses and to various natural habitats and climate changes is an emerging and urgent goal, as outlined in the Plant Science Decadal Vision 2020–2030 (Henkhaus et al., 2020). In particular, Decadal Vision's proposed actions include, among others, the selection of ecologically diverse plant lineages for an in-depth analysis of their morphology, anatomy, ecology in their natural environments, as well as the exploration and characterization of as-yet-undiscovered plant-associated biota. In the context of Fe nutrition, the issues raised by Plant Science Decadal Vision suggest that the adapting processes of non-crop plants to calcareous habitats can

potentially uncover traits lost in domesticated crops. Moreover, they also support the importance of studying the root microbiota associated with non-crop plants (or wild crop relatives). Interestingly, urban calcareous habitats can also constitute a potential source of information of the resilience of plants in inhospitable soils.

In most cases, crop domestication led to modifications of the composition of root microbiota, with adverse effects on the association with beneficial plant microbes (Perez-Jaramillo et al., 2016). Root exudation of metabolic compounds plays a crucial role in influencing the recruitment of functional microbiota. In general, the variety of biotic and abiotic stresses, such as Fe deficiency, encountered by plants during *in vitro* and *in vivo* growth conditions impacts the biosynthesis of secondary metabolites (Cheynier et al., 2013; Isah, 2019). Several works have reported an increased number of phenolic compounds in plants and root exudates as a response to different environmental stresses (Cesco et al., 2010; Caretto et al., 2015), and as an adjustment of secondary metabolism occurring in response to Fe mobilization (Jin et al., 2007). Some species, such as *P. judaica*, can secrete ortho-dihydroxy phenolic compounds showing reducing and metal chelating properties that enhance Fe availability in the rhizosphere. Indeed, plant metabolites released to rhizosphere can have diverse effects on soil microbial com- munities by changing soil properties or nutrient availability in the root vicinity, directly attracting microbes or being toxic for others (Vive- s-Peris et al., 2020).

In some cases, specific plant root exudates initiate a molecular dialogue mediated by both partners' exometabolite production, resulting in the establishment of beneficial plant-microbe associations (Sasse et al., 2018). Badri and co-workers found a strong positive correlation between phenolics and Plant Growth Promoting Bacteria (PGPB) species, including *Rhizobium*, *Bacillus*, *Sphingomonas*, *Streptomyces* and *Frankia* (Badri et al., 2013). A similar mechanism of recruitment of PGPB has been demonstrated for coumarins in Fe-limiting soils: besides their established role in Fe mobilization in the rhizosphere (Rajniak et al., 2018), coumarins are also involved in shaping root-associated micro- biomes (Voges et al., 2019). Furthermore, Harbort et al. (2020), by using synthetic microbiota and *A. thaliana* plants deficient in the exudation of secondary metabolites, demonstrated that coumarins are important drivers for the assembly of the rhizospheric bacterial community under Fe deprivation. All these recent works on the tripartite interaction be- tween roots' exudates, soils and microorganisms support the emerging view that metabolites exuded under peculiar environmental conditions can recruit microbiota components able to alleviate the specific stress experienced by the plant.

The present work aims to unravel root-related processes of *Parietaria judaica*'s response to Fe

deficiency, and particularly its root plasticity and metabolite exudation under Fe deficiency. *P. judaica* (L. 1753) is a wild perennial dicotyledonous plant capable to grow in acidic and alkaline soils (Tato et al., 2020); it represents the most widespread plant species found in highly calcareous and hostile environments such as wall cracks exposed to the sun, where it displays phenotypic changes, though without any chlorosis symptoms (Dell'Orto et al., 2003; Donnini et al., 2012; Tato et al., 2020). In this work, we adopted a field-to-lab approach to first investigate the microbiome associated with *P. judaica* roots in plants growing spontaneously in an urban environment and harvested from an extremely calcareous habitat. We then analyzed phenolics content and root plasticity and exudation in *P. judaica* plants grown under various controlled laboratory conditions mimicking the effects of calcareous environments; in particular, we applied conditions that allowed us to discriminate the effects of low Fe availability from those caused by the presence of carbonate and alkaline conditions (Tato et al., 2020).

Material and methods

P. judaica growth conditions

P. judaica plants were sampled in an urban area of Milan (45°28′36.8′′N, 9°13′39.2′′E; 45°28′37.0′′N, 9°14′00.1′′E; 45°28′35.2′′N, 9°14′03.7′′E): to sample the whole root apparatus, the walls and the substrates where plants were growing were broken if necessary.

Cuttings of *P. judaica* were allowed to radicate in aerated half- strength nutrient solution for 10 days (Tato et al., 2020). Rooted plants were then transferred into 10 L plastic tanks (40 plants/tank) under four different conditions: +Fe (control, complete nutrient solution adjusted to pH 6.2 with NaOH), -Fe (complete nutrient solution without Fe, adjusted to pH 6.2), Bic (complete nutrient solution supplemented with 5 mM $CaCO_3$ and 15 mM $NaHCO_3$, pH 8.3) and Tric (complete nutrient solution, buffered with Tricine at pH 8.3); the pH was adjusted with NaOH if required. The nutrient solution was changed every two days. Plant size at the harvesting time has been previously reported in Tato et al. (2013).

Treatments were carried out for 7 days in a growth chamber under 16/8 h light/dark regime with cool-white light 200 µmol photons m^{-2} s^{-1}, 27/21 °C temperature range, 65–75% relative humidity.

Sampling of P. judaica in urban sites and DNA extraction of their root-associated microbes

From each of the three urban sampling sites considered, three replicates of bulk soil (i.e. the soil portion not affected by the root presence, according to Bulgarelli et al., 2012) and root samples from *P. judaica* were collected. Large soil aggregates were removed from the roots by shaking as described in Bulgarelli et al. (2012), in order to leave only the (rhizospheric) soil attached to the roots. Bulk soil and root samples with attached soil were then stored at −20 °C until DNA extraction. To obtain the samples that represent the root-associated microbial diversity, the root-adhering soil plus the root itself were processed together. This condition accounts both for the externally associated microbes and for the root endophytes (the rhizosphere + the endorhiza, called rhizosphere for the sake of brevity hereinafter).

The rhizosphere samples were first lyophilized for 24 h and then ground to a fine powder with liquid nitrogen. DNA was obtained as described in Edwards et al. (2015) extracting from a 300-mg bulk soil samples and 50 mg rhizospheric samples (dry weight), by using the MoBio PowerSoil DNA Isolation Kit (Qiagen Inc., Hilden, Germany) and DNeasy Plant Mini Kit (Qiagen Inc., Hilden, Germany), respectively, according to the manufacturer's instructions.

Extracted DNA was quantified using NanoDrop spectrophotometry (NanoDrop, Wilmington, DE, USA) and normalized prior to library construction for the high-throughput sequencing.

Molecular, bioinformatic and statistical analyses of the microbes associated with P. judaica roots

The extracted genomic DNA was used to amplify the V3–V4 region of the prokaryotic 16S rRNA gene, using the modified primer pair pro341f/ pro805r (Takahashi et al., 2014) with the standard Illumina overhang. Fungal ITS2 rDNA cistron was amplified using the modified primers fITS7 (Ihrmark et al., 2012) and ITS4ngs (Tedersoo et al., 2014), with the standard Illumina overhang adapters. Purified PCR products were combined in equimolar amounts, and the corresponding metabarcoding libraries were sequenced on the Illumina MiSeq platform (Illumina, San Diego, CA, USA) with paired-end 2 × 300 bp sequencing mode at the IGA Technology Services (Udine, Italy).

Raw data were processed and analyzed following the pipelines of QIIME2 version 2019.7.0 (Bolyen et al., 2019; Caporaso et al., 2010). The high-quality reads were clustered into operational taxonomic units (OTUs) at a 97% identity level and chimeric sequences were filtered using UCHIME (Edgar et al., 2011), as implemented in the QIIME2 pipeline. Taxonomy assignment of both prokaryotic and fungal OTUs was performed using the

SILVA database (version 132, release date December 13, 2017; Quast et al., 2012; Yilmaz et al., 2013) and the ITS UNITE database (UNITE QIIME release for Fungi, Version November 18, 2018. https://doi.org/10.15156/BIO/786334) respectively using *sklearn* algorithm as implemented in QIIME2 (Pedregosa et al., 2011).

All statistical analyses were conducted in R v3.6.1 (R Development Core Team, 2016). Rarefaction species richness curves were generated using the R package *vegan* (Oksanen et al., 2013). Alpha diversity in- dexes were calculated for Prokaryotic and Fungal OTU tables using the *vegan* package (Oksanen et al., 2013). The differences between soil and root samples were tested by using Tukey's Honest Significant Differences test, with the R package *TukeyC* (Faria et al., 2016).

To correct for difference in sequencing depth, a subsampling at even sequencing depth from each sample (9935 for Prokaryotic and 2632 for Fungal samples) was performed before the downstream analysis using the R package *phyloseq* (McMurdie and Holmes, 2013), generating also the taxonomical composition of the whole microbial community. The significance of Bray-Curtis dissimilarity between the soil and root samples were tested by permutational multivariate analysis of variance (PerMANOVA) using the *adonis* function in the R package *vegan* with 9999 permutations. The multivariate homogeneity of group dispersions was first assessed by means of the *betadisper* and *permutest* (with 9999 permutations) functions in the R package *vegan*. The differences in the composition of Prokaryotic and Fungal communities in *P. judaica* soil and root samples were visualized by means of a Non-metric Multidimensional Scaling (NMDS) ordination carried out using *metaMDS* function in the R package *vegan*. The R package *gunifrac* (Chen et al., 2012) was used to test differences in the microbial composition of soil and root samples. Co- occurrences in the Prokaryotic and Fungal com- munities were assessed by performing network analysis using the Spearman rank correlations between OTUs ($\rho > 0.7$ and $p < 0.001$). All networks were visualized with the Fruchterman-Reingold layout with 9999 permutations in the R package *igraph* (Csardi and Nepusz, 2006). Descriptive and topological network properties, as well as network modules (substructures of nodes with a higher density of edges within the group than outside it) were calculated as described in Hartman et al. (2018).

Morphological analysis of arbuscular mycorrhizal (AM) root colonization

Roots of *P. judaica* plants sampled in urban sites (described above, $n = 8$) were carefully washed with tap water, stained overnight in a solution of methyl blue (0.1% w/v) in 80%

lactic acid (v/v) and clarified in lactic acid in order to remove the excess of staining solution. 80 segments, 1 cm long each, were obtained from each root apparatus, placed on glass slides and observed under a light microscope.

HPLC analysis of phenolic compounds

For qualitative and quantitative determination of phenolic com- pounds, plant tissues (1 g FW) of *P. judaica* were first homogenized for 3 min with 30 mL hot MeOH–EtOH (1:1) and then refluxed under nitrogen for 30 min (2 ×). After centrifugation and pooling of the extracts, the combined solutions were first concentrated under vacuum, depigmented with petroleum ether (bp 40–70 °C), filtered through 0.45 µm Millipore Millex-HN, and then used for the determination of total phenolic content and HPLC-DAD determination of phenolic compounds (Lattanzio et al., 2001). Identification of phenolics was made by using retention times (tR) and spectral data of different peaks compared with standard com- pounds (Extrasynthese, Genay, France). In addition, HPLC-MS/MS analyses of main peaks identified in *P. judaica* and standard compounds were used for structure characterization. Metabolites released by root (root exudates fraction) were collected according to Tato et al. (2020) from plants grown hydroponically. The collected materials were acidified to pH 3.5–4.0 with HCl to maintain the structural stability of phenolic compounds, freeze-dried, suspended in 3 mL methanol and filtered through 0.45 µm Millipore Millex-HN; the filtered solution was analyzed for total phenolic content and HPLC determination of phenolic compounds. HPLC analyses were performed with Hewlett Packard Series 1100 liquid chromatograph equipped with a binary gradient pump G1312A, a G1315A spectrophotometric photodiode array detector was set at 325 nm, and G1316A Column with the thermostat set at 45 °C. The Hewlett Packard Chem Station (Rev. A. 06.03) software was used for spectra and data processing. An analytical Phenomenex (Torrance, CA, USA) Luna C18 (5) column (4.6 × 250 mm) was used throughout this work. The solvent system consisted of (A) MetOH and (B) acetic acid-water (5/95, v/v). The elution profile was as reported by Lattanzio and Van Sumere (1987). The flow rate was 1 mL min^{-1}. Samples ~~of~~ (25 µl) were applied to the column using a 25 µl loop valve. UV absorption spectra were acquired in the 235–450 nm range.

HPLC-MS/MS analyses were performed on a QTrap MS/MS system, (Applied Biosystems, Foster City, CA, USA), equipped with an ESI interface and a 1100 series micro-LC system comprising a binary pump and a microautosampler (Agilent Technologies, Waldbronn,

Germany). The ESI interface was used in positive ion mode, with the following settings: temperature (TEM) 350 °C; curtain gas, nitrogen, 30 psi; nebuliser gas air, 10 psi; heater gas, air, 30 psi; ion spray voltage + 4500 V. Full scan chromatograms were acquired in the mass range 100–800 amu, MS/MS chromatograms were acquired at collision energy of 20 V. LC conditions were as for the HPLC-DAD analysis.

Root morphology and biomass allocation

After 7 d treatments (+Fe, -Fe, Bic, Tric), three independent bio- logical samples from each treatment were collected randomly, and their shoots and roots were harvested. Shoots were dried at 70 °C for 48 h, and their dry weight (WS, g) was measured. The root system was stained with 0.1% (w/v) toluidine blue O for 5 min and then divided into two root orders: 'shoot-borne' or adventitious roots (AR), and their 1st- order lateral roots (LR) as defined by Atkinson et al. (2014). Each root was scanned at 300 dpi resolution (WinRhizo STD 1600, Instruments Regent Inc., Canada) to determine length (LA, cm), volume (VA, cm^3) and surface area (SA, cm^2) of the adventitious roots and total length (LI, cm), total volume (VI, cm^3) and total surface area (SI, cm^2) of the 1st-order laterals using the WinRhizo Pro v. 4.0 software package (Instruments Regent Inc.). Length (LT), surface area (ST) and volume (VT) of the whole root system were calculated as the sum of the two root types. Then, dry weights of the adventitious roots (WA, g) and total dry weight of 1st-order lateral roots (WI, g) were measured after drying in an oven at 70 °C for 48 h. Total root dry weight (WT, g) was the sum of the WA and WI. Plant dry weight (WP, g) was obtained as the sum of WT andWS. Based on the measurements above, the following parameters were calculated for the whole root system:

root length ratio RLR = LT/WP ($cm\ g^{-1}$)

root mass ratio RMR = WT/WP ($g\ g^{-1}$)

fineness F = LT/VT ($cm\ cm^{-3}$)

tissue density TD = WT/VT ($g\ cm^{-3}$)

where RLR expresses the root order's potential for the acquisition of below-ground resources, the RMR indicates the relative biomass allocated to the root and F and TD represent the structural root parameters. The relationship among these parameters is: RLR = RMR x F/TD (Ryser and Lambers, 1995).

The adventitious (NA) number and the 1st-order laterals (NI) were directly counted from the images. The average length of the adventitious [aLA = LA/NA] and the 1st-order laterals [aLI = LI/NI] (cm) were also calculated (Table S1). The 'branching zone' length (BZ) that extends rootwards from the shoot base to the youngest emerged LR and the 'lateral formation zone' (LFZ) that spreads from below the youngest emerged LR up to the 2–6 mm from the root apex were also measured, as described in Dubrovsky and Forde (2012). NI/BZ calculated the root branching density (BD, number of laterals in cm of branching zone).

Two-way ANOVA tested the effects of the different treatments on the root parameters. Tukey's post hoc test comparison was applied to test the effects of each treatment at $P < 0.05$. To correct for allometric effects (Coleman et al., 1994), the ln-transformed plant dry weight (ln WP) was used as a covariate to analyze the root morphology and biomass allocation, when significant correlations between lnWP and these root traits were found. A multivariate statistical PCA (principal components analysis) and a cluster analysis were performed using SPSS software. To unveil the impact of the root morphology pattern on plant growth, Pearson's test was used to test the correlation between the PC factor scores and plant DW. Statistical analysis was conducted using the Systat v. 8.0 software package (SPSS Inc., Evanston, IL, USA).

Estimation of total ortho-dihydroxy phenolic compounds (Arnow's reagent)

One mL of extract sample was placed in a test tube and 1 mL 0.5 N HCl was added. The tube was well mixed and then 1 mL Arnow's reagent (10 g Na nitrite and 10 g Na molybdate in a final volume of 100 mL distilled water) was added (which resulted in a yellow color), mixed, and 1 mL 1 N NaOH was added (solution turned into red color). The solution was then brought to a final volume of 5 mL with distilled water and absorbance was measured at 500 nm. The concentration was calculated and expressed as mg g^{-1} FW. Chlorogenic acid was used as a standard, in a range of 0–0.15 mg mL^{-1}.

Iron reduction by phenolics compounds

The phenolics concentration in root exudates and the caffeic and citric acids ability to reduce Fe(III)-EDTA was measured spectrophotometrically by using BPDS (Chaney et al., 1972). Root exudates (100 µg), prepared as described above, were incubated for 120 min in 1 mL 100 mM Fe(III)-EDTA, 100 mM BPDS solution, in the dark, at 26 °C and under

shaking. A solution containing caffeic (50 mM) and/or citric acid (50 mM), 100 mM Fe(III)-EDTA and 100 µM BPDS, in the dark at 26 °C and under shaking, was also prepared, according to Hu et al. (2005). The absorbance at 535 nm was measured as in Donnini et al. (2009).

Soil incubation with caffeic and citric acids

Solutions of caffeic and citric acids were adjusted to pH 5.5 using diluted NaOH and added to soil at rates 50 µmol acid g^{-1} soil according to Hu et al. (2005). The soil was watered to field capacity, and then incubated at 20 °C for 30 min. Soluble soil fractions were collected ac- cording to Mimmo et al. (2008). Extracts were filtered through 0.2 µm filters and then analyzed by an Agilent 7100 Capillary Electrophoresis System (Agilent Technologies, Santa Clara, CA, US). Phosphate anions were determined by capillary electrophoresis, using a bare fused silica capillary with extended light path BF3 (i.d. = 50 µm, I = 72 cm, L = 80.5 cm). Sample injection was at 50 mbar for 4 s with —30 kV voltage and detection at 350/80 nm wavelength. Compounds were identified using pure standards and anion contents were expressed as µg g^{-1} FW.

Miscellaneous

Iron and P content were determined by ICP-MS on oven-dried tissue samples (n = 3) mineralized in HNO_3. and carboxylic acids contents in roots were determined according to Tato et al. (2020). Apoplastic Fe was determined according to Tato et al. (2020). Briefly, roots from 5 plants per treatment were transferred to a beaker with 0.5 mM $CaSO_4$ under vigorous aeration. After 10–15 min, roots were transferred to 40 mL tubes with 21 mL of 10 mM 2-(N-morpholino)-ethanesulfonic acid (MES), 0.5 mM $Ca(NO_3)_2$, 1.5 mM 2,2' bipyridyl (pH 5.5) at 25 °C. Tubes were covered with a cotton plug and N_2 was bubbled through the solution. After 5 min, 1 mL of 250 mM $Na_2S_2O_4$ was added. The A_{520} of the solution (Fe[bipyridyl]3 ε = 8.650 M^{-1} cm^{-1}) was determined on 2 mL aliquots. The aliquots employed for the determinations were returned to the tube and left for 1 h in the dark. The determination was carried out every 1 h 30 min until a constant value was obtained. Lignin visuali- zation was performed according to Donnini et al. (2011). After being fixed at 4 °C overnight in 100 mM Na-phosphate buffer (pH 7.00) containing 4% paraformaldehyde (w/v), root segments were dehydrated through an ethanol–tertiary

butanol series and embedded in paraffin (Paraplast Plus, Sigma). Serial sections (5 µm) were cut with a micro- tome, mounted on silanized slides, deparaffinized in xylene and rehydrated through an ethanol series. Sections were then stained with the safranin/fast green method (Johansen, 1940), mounted with cover slides, observed by optical microscopy (Leica DMR) and images were acquired using a digital camera (Leica DC300F).

Results

The root-associated microbiome of P. judaica collected from urban sites

P. judaica plants were harvested from soil of an urban site displaying alkaline and calcareous conditions, with a pH value of 7.9 ± 1.3 and an average 20% $CaCO_3$ content. The root-associated microbiota of the collected plants (rhizosphere samples) and that of the soil not affected by the root presence (bulk soil samples) were then analyzed. The rarefaction curves indicated that a satisfactory sequencing depth was obtained for each considered sample, for both fungal and bacterial amplicons (Fig. S1). The clustering of high-quality reads allowed us to obtain 349 fungal and 2327 prokaryotic operational taxonomic units (OTUs), that were further assigned taxonomically (Supplemental files 1a, 1b). The standardized datasets were used to generate Venn diagrams of the community composition and unique or shared OTUs among bulk soil and rhizosphere samples (Fig. 1). The results show a reasonable degree of microbiota diversity, especially for prokaryotes (more than 2000 OTUs overall). Also, a lower number of OTUs unique to the rhizosphere compartment was detected, while the highest OTU number was present in the bulk soil only. The OTUs shared between rhizosphere and bulk soil likely represent the core of microbes recruited by roots under the occurring environmental conditions.

The analysis of Alpha diversity indexes outlines the structure of the considered microbial communities (Fig. S2). All indexes point to a higher microbial richness in the bulk soil than the rhizosphere, in agreement with the higher OTU number detected in the former compartment. A general analysis of Beta diversity on prokaryotic and fungal communities was also conducted. The Bray-Curtis index did not find a significant dissimilarity in the microbial composition of bulk soil and rhizosphere; however, the two compartments appear more diverse when phylogenetic distances weighted by relative abundances were considered in relation to fungal microbiota (weighted GUnifrac, Fig. S3). Notably, the prokaryotic taxa typically present and dominant in soils (Jansenn, 2006) were all detected in the current experiment (Fig. 2), with Proteobacteria as the most represented in both compartments. However, Acidobacteria were underrepresented; this result is consistent

with the high pH of the soil under investigation (around pH 7.9), as many species in this phylum are indeed acidophilic.

The bulk soil and rhizosphere compartments do not show a dramatic difference in the overall community structure, although some shifts in microbial composition can be detected already at the phylum level (Fig. 2). The rhizosphere showed an increase in the relative abundance of Proteobacteria, Actinobacteria and Firmicutes phyla in comparison to the bulk soil. In contrast, other phyla such as Bacteroidetes, Chloroflexi, Planctomycetes and Verrucomicrobia were significantly more abundant in the bulk soil compartment than in the rhizosphere (Fig. 2, upper panel).

A more in-depth analysis of microbiome composition (at genus level) revealed a higher relative abundance of Bacillus, the Rhizobium group and Streptomyces in the rhizosphere, and for the last two genera the increase was statistically significant (Fig. 3, upper panel). However, the fungal genera Mortierella and Wallemia were more abundant in the bulk soil (Fig. 3, lower panel). This latter genus comprises a few known species for their xerotolerant and halophilic behaviour (Zajc and Gunde-Cimerman, 2018).

Arbuscular mycorrhizal (AM) fungi provide many services to plants, including the improvement of mineral nutrition, at a cost for the plant host, since they take up photosynthates from the roots. Hence, the presence of AM fungi of such urban soil was also investigated; a few OTUs referring to AM fungi were retrieved in both the bulk soil and the rhizosphere compartment (data not shown). They point to *Funneliformis mosseae*, a widespread species common in diverse soils, and to another AM fungus also belonging to Glomeromycotina. Despite AM OTUs not being abundant in our dataset, arbuscule formation was observed in the same *P. judaica* roots sampled for the microbiome sequencing, suggesting that AM fungi are an active microbial component of such an urban niche.

Co-occurrences in the Prokaryotic and Fungal communities were assessed by performing network analysis and visualising the positive, significant correlations among OTUs ($\rho > 0.7$ and $p < 0.001$, Fig. S4). Similarly, meta-networks were constructed to visualize correlations between Prokaryotic and Fungal OTUs in the soil and root communities (Fig. 4). Within this network, we identified keystone OTUs (Fig. 4), defined as the top 1% node with the highest degree of interactions. These OTUs are microbial taxa that frequently co-occur with other taxa under the experimental conditions considered, and are thought to be ecologically important and to play potentially a key role in the structuring of the microbiota (Hartman et al., 2018, Supplemental file 2).

Also, OTUs that might act as indicator species in such networks were sought; a species is described as an "indicator" when it is characteristic of a group of samples or experimental treatments and/or is highly sensitive to the changes entailed by the treatment. Only two bacterial OTUs could be identified as indicators for the rhizosphere compartment (Supplemental file 3): the first one refers to the Rhizobium genus (probably *Rhizobium grahamii*, 100% sequence identity), the second points to an uncultured isolate belonging to Actinobacteria (99.75% identity). Members of Actinobacteria are widespread in soils and display tolerance to diverse extreme conditions (Ranjani et al., 2016).

Indicator species of the bulk soil comprise genera of fungi and bac- teria known to be widespread in soils, including saprotrophs such as Mortierella as well as microbes that tolerate extreme environments, such as the fungi *Coniosporium apollinis* and *Naganishia albida*, as well as the bacteria Microvirga, Brevundimonas, Altererythrobacter and Rhodo- spirellula (Supplemental File 3).

The microbiome associated with the roots displayed an increase in P solubilizing microbial genera (as defined by Kalayu, 2019), mainly belonging to Rhizobiaceae and Streptomyces (Fig. 3, upper panel). Conversely, some soil generalist microbes seem to be rather excluded from the rhizosphere of *P. judaica*.

Root morphology of P. judaica grown in calcareous, alkaline or Fe- deprived media

P. judaica plants sampled from the urban sites were allowed to radicate in half-strength complete nutrient solution and then transferred into one of four different media (i.e. +Fe, -Fe, Bic and Tric), to discriminate between the effects of low Fe availability due to a high pH and those of bicarbonate itself (Tato et al., 2020). Since alkaline and calcareous conditions mainly affect Fe and P availability, the leaf and root concentration of these nutrients was determined. A reduction of Fe concentration was observed in leaves of plants grown in the -Fe, Bic and Tric media, and in -Fe roots (Fig. 5). Phosphorus was slightly decreased with respect to the control only in the roots of plants grown in Bic (Fig. 5).

The morphology of the whole root systems of *P. judaica* was not significantly modified by all the treatments in comparison with the +Fe condition, with exception of the TD (Fig. 6A, B and C). Indeed, the TD of the whole root system was lower in the -Fe and +Fe than in Bic- and Tric- treated plants (Fig. 6C).

The root system of *P. judaica* consisted of the adventitious roots (AR), also named "shoot-borne" roots, and the lateral roots (LR), which emerged from AR, suggesting the "within-root" approach to analyze the root morphology. Differently from the whole root system, some

treatments significantly modified the LI, the aLI and the aLA in comparison to those of the +Fe plants (Fig. 6D): Bic-treated plants decreased (—49%) the aLA in comparison to the +Fe treatment and the Tric treatment reduced the LI and aLI by —83% and —71%, respectively, compared to the +Fe plants (Fig. 6D). The Fe-deficient plants exhibited similar morphology in both root types when compared with the +Fe plants (Fig. 6D). As expected in plants adapted to alkaline soils (White et al., 2013), Bic-treated *P. judaica* plants exhibited an increase in the BD (+61%) associated to a reduction of the BZ, but these parameters were unchanged in the Fe deficiency and Tric treatments (Fig. 6E).

The PCA was applied using only root parameters significantly changed by treatments as observed in the univariate ANOVA. The PC1 (explaining 49% of the variance) consisted of high positive loads for the aLA and the BZ and negative loads for the TD, while the PC2 (explaining 38% of the variance) showed high positive loads for the LI and aLI (Table 1). Two-dimensional PCA score plots and subsequent hierarchical cluster analysis revealed a sharp separation among the treatments (Fig. 6A; Fig. S1). In particular, a first cluster included the +Fe plants, a second cluster comprised the Bic-treated plants, and a third one incorporated both the Tric- and Fe deficient-treated plants (Fig. 7A; Fig. S5). As shown by Fig. 6A and Table 1, the Bic-treated plants were characterized by lower aLA and BZ associated with high TD, aLI and LI, thus exhibiting root architectures different to the +Fe plants. Conversely, the root architectures of the Fe deficient- and Tric-treated plants exhibited lower aLI and LI but intermediate values of aLA, RBZ and TD between the Bic treated and the +Fe plants (Fig. 6A). The importance of these different root architectures for the *P. judaica* fitness was tested by a Pearson correlation between the plant dry weight and the PC1 and PC2 scores. The PC1 was significantly and positively correlated with the plant growth ($r = 0.4890$, $p = 0.0139$) differently to the PC2 ($r = 0.0356$, $p = 0.55$) (Fig. 7B and C), suggesting that the high aLA, BZ and low TD but not the lateral roots (PC2) explained most of the *P. judaica* growth.

Carboxylic acids and phenolic compounds in root tissues and in exudates of P. judaica grown in calcareous, alkaline or Fe-deprived media

The total phenolics and carboxylic acids released by *P. judaica* roots were recently monitored in the four conditions, i.e. control, -Fe, Bic, Tric (Tato et al., 2020). The profile of carboxylic acids and the total phenolics of *P. judaica*, both in roots and in their exudates are shown in

Figs. S6 and S7, respectively. Malic, ketoglutaric and citric acids were detected in all tested root samples, with a higher accumulation of malic and citric acid in -Fe, Bic, and Tric treatments, whereas ketoglutaric acid con- centration increased only in -Fe and Tric-treated plant roots. Both malic and citric acids were present in all root exudates, with a higher accumulation in -Fe, Bic and Tric treatments. Notably, cis-aconitic acid was exuded only by the Tric-treated roots.

Total root phenolics were measured spectrophotometrically using Arnow's reagent, which selectively determines the concentration of ortho-dihydroxy phenolic compounds (Fig. S7A). Only the Bic treatment induced a significant increase (87%) of total phenolic concentration in roots. A non-significant increase was observed in the other two conditions, -Fe and Tric (+28% and +17% respectively). These data are consistent with the results obtained from chromato- graphic HPLC-MS analyses where an increase of total phenolics in plants grown under Bic condition (+73%) and in plants grown in Tric conditions (+18%) was found (Fig. S7B). In detail, the phenolic fraction of root tissues was characterized by the presence of various positional isomers of mono- and di-caffeoylquinic acid esters. 5-*O*-caffeoylquinic acid (chlorogenic acid) and 3,5-*O*-dicaffeoylquinic acid were the main constituents of the phenolics fraction in root extracts (Fig. 8A, left panel). Other caffeoylquinic derivatives identified in roots were: 3-*O*- caffeoylquinic acid, 4,5-O- and 3,4-O-dicaffeoylquinic acids, and two *p*-coumaric acid glycosides. Accordingly, the phenolics content of plants harvested in the urban site revealed that the main constituents of root extracts of *P. judaica* were represented by chlorogenic acid and 3,5-O- dicaffeoylquinic acid, which constitute together about 88% of the total phenolic compounds present in root extracts (Fig. 8B).

From a qualitative viewpoint, isomerization phenomena have been observed in the phenolic fraction of stressed plants in comparison with the control. Overall, such isomerization phenomena in all stressed plant extracts was associated to an increase of total mono-caffeoylquinic acids while the total content of di-caffeoylquinic acids decreased (Fig. 8A, left panel).

The nutritional stress conditions -Fe, Bic, Tric also affected the composition of phenolic fractions of *P. judaica* root exudates (Fig. 8A, right panel) in which 3-*O*- and 5-*O*-caffeoylquinic acids, 3,5-*O*-dicaffeoylquinic acid and the caffeic acid aglycone were identified; the latter compound is absent in root extracts. This suggests that secretion of phenolics by *P. judaica* roots (both control and stressed roots) also leads to partial hydrolysis of caffeoylquinic esters. Although total phenolics concentration determined by Arnow's reagent method revealed an in- crease mainly in root exudates of -Fe plants (Fig. S7A), HPLC-MS results revealed an

increase in total phenolics root exudates from -Fe, Bic and Tric treated plants (Fig. S7B). Again, the highest increase in phenolics was observed in Bic exudates.

In Bic and Tric exudates, caffeic acid accounted for 67 and 44% of the total phenolics, respectively. Caffeic acid and chlorogenic acid together accounted for 76–84% of total phenolic compounds in both control and all the stressed exudates (Fig. 8A, right panel).

Fe mobilization properties of P. judaica's root exudates in calcareous, alkaline or Fe-deprived media

The ability of root exudates to favor Fe mobilization was tested by measuring the *in vivo* Fe reductase activities of exudates secreted from roots of *P. judaica* plants grown in -Fe, Bic and Tric media. Such Fe reductase activity was increased by all three stress conditions, and in particular, it was the highest in the Bic treatment (Fig. 9A). Since Bic- grown *P. judaica* roots exuded citric and caffeic acids, the effect of commercially available caffeic and citric acids on the Fe(III) reduction was assayed. Caffeic acid displayed a higher Fe reduction capacity compared with citric acid (Fig. 9A). Besides Fe availability, calcareous conditions also affect phosphorus (P) availability; the urban calcareous soil where plants were collected was incubated with caffeic and citric acid to study their potential effect on PO_4^{3-} solubility. Soil incubation with both caffeic and citric acid enhanced the concentration of PO^{3-} in the soil soluble fraction with respect to the control, but the effect of citric acid was stronger than that of caffeic acid (Fig. S8).

Bic treatment led to a significant accumulation of Fe in the apoplast, suggesting that the higher synthesis of phenolics compounds might be induced by the high Fe content in the intercellular spaces (Fig. 9B). Other than Fe mobilization, phenolics might be involved in other re- actions, such as lignification process (Donnini et al., 2011). Therefore, the lignification rate of root tissues was investigated by a staining procedure and the root cross-sections were visualized microscopically. Roots of plants grown under Bic and Tric showed high lignification signals at rhizodermis, endodermis and cortex layers (Fig. 9C). Such findings suggest that both alkaline growth conditions (Bic and Tric) induced the synthesis of lignin in the root cell walls.

Discussion

The study of plants living in natural and extreme environments, in which different stressors naturally coexist, allows to unravel the morpho-anatomical and physiological traits enabling them to survive in these extreme environments (Bartoli et al., 2013; Bechtold,

2018). In this paper, we investigated different traits characterizing the root-soil interaction of *P. judaica*, a wild plant species commonly known as "Pellitory of the wall", including morphological plasticity, exudation, and association with the microbiome.

The analysis of the root microbial community associated to spontaneous *P. judaica* plants harvested from the urban environment revealed a good degree of microbiota diversity, detecting all prokaryotic taxa typically present and dominant in soils. The comparison of the root-associated versus bulk soil microbiota highlighted some shifts in the microbial composition, with a higher relative abundance in the rhizo- sphere of some genera, including beneficial species for plants. Among these beneficial bacterial species, two OTUs are noteworthy; the first OTU refers to a bacterium from the genus *Rhizobium*, whereas the second OTU points to an unidentified actinobacterium. Besides the Rhizobia's ability to form N-fixing nodules on legume roots, they can also thrive in the rhizosphere of non-leguminous plants acting as Plant Growth Promoting Rhizobacteria (PGPR, Mehboob et al., 2012), thus providing benefits even in the absence of nodule formation. Also, besides the well-studied *Streptomyces* genus, many other Actinobacteria can associate with roots of a wide range of hosts beneficial for the plants' health, and the interest in their use as PGPR bacteria has raised in recent years (Sathya et al., 2017).

Taken together, our analyses of the root-associated microbiome of spontaneous urban *P. judaica* plants indicate that these plants retain the competence to actively recruit beneficial soil microbes such as PGPR, phosphate solubilizers and AM fungi, possibly excluding from their rhizosphere other components of the soil microbiota. These results are remarkable, given the limited microbial reservoir to which plant roots had access in the urban environmental niche where these plants were growing.

It is now well acknowledged that plants play an active role in the assembly of the rhizospheric microbiota, and the outcome and magnitude of such an influence can change, depending on both fixed (e.g. plant genotype) and variable (biotic/abiotic stresses) factors. In this scenario, root exudation can act as a crucial driver of microbiota recruitment (Sasse et al., 2018). Among the different fractions of *A. thaliana* root exudates, phenolics are very effective in shaping the soil microbiome, as they significantly correlate with 31 bacterial OTUs (Badri et al., 2013). Also, a role for root-secreted coumarins in shaping the *A. thaliana* rhizospheric microbiota has been found (Voges et al., 2019). In particular, coumarins limit the growth of a *Pseudomonas* strain through a mechanism that involves the production of reactive oxygen species. Interestingly, we could not highlight any significant enrichment for the *Pseudomonas* genus in the *P. judaica* rhizosphere, although some other genera of PGP bacteria seemed to be actively recruited in the rizhoplane. This suggests that

571 the negative effect demonstrated for coumarins on *Pseudomonas* growth might be extended
572 to other phenolic compounds, thus providing indications towards the engineering of
573 beneficial plant root microbiota.
574 Root morphological plasticity and exudation, which are two relevant processes driving
575 plant-soil interaction, were investigated in *P. judaica* grown in three different controlled
576 conditions inducing Fe-deficiency, i.e. -Fe, Bic, Tric, to discriminate between root
577 responses to the low availability of Fe due to a high pH and that caused by bicarbonate
578 (Tato et al., 2020). Among the morphological parameters of the whole root system, the TD
579 of *P. judaica* was the only affected trait, mainly by the calcareous condition (Bic) (Fig.
580 1C). The TD is an adaptive trait positively correlated with the lignification degree and cell
581 wall thickness (Ciamporova et al., 1998; Wahl and Ryser, 2000; Hummel et al., 2007) and,
582 in turn, is inversely related to the *Arabidopsis* adaptation to Fe deficiency (Barberon et al.,
583 2016). As well, the root lignification degree has been interpreted as a Fe deficiency
584 sensitivity trait in a quince rootstock (Donnini et al., 2011).
585 Besides studying the morphology of the whole root system, a 'within- root analysis' was applied,
586 looking at the morphological changes of the different root types. Such a phenotyping
587 approach could provide early information on the contributions of the different root types of
588 *P. judaica* to the adaptation in alkaline, calcareous and Fe deficient conditions. Indeed, root
589 types were found to respond differently to the environmental cues such as water (Romano
590 et al., 2013; Tellah et al., 2014; Abenavoli et al., 2016), salt (Stevanato et al., 2013), and
591 combined P/drought stress (Ho et al., 2005), N deficiency (Sorgona` et al., 2007),
592 allelochemicals (Abenavoli et al., 2004, 2008; Lupini et al., 2016), as well as rot (Roman-
593 Aviles et al., 2004) and fungal colonization (Zad- worny and Eissenstat, 2011). In the
594 present work, lateral roots of *P. judaica* were more modified by treatments than
595 adventitious ones. This kind of root ideotype, which is characterized by an even extended
596 spread of roots throughout the soil, is useful for the acquisition of nutrients with restricted
597 phytoavailability in alkaline soils (White et al., 2013). Indeed, *P. judaica* exhibited an
598 increase of the BD (+61%), maintaining the LI, in response to the Bic treatment (Fig. 5D
599 and E).
600 Recently, several works pointed out the importance of the synergism and/or antagonism
601 among the different root traits for understanding the root architecture adaptation to diverse
602 environments (York et al., 2013; Miguel et al., 2015; Rangarajan et al., 2018), suggesting
603 using a multivariate rather than a univariate approach for analyzing *P. judaica* root
604 architecture. The "root multi-trait" pattern, as determined in the present work, also in
605 agreement with the results of within-root morphology, might reflect the adaptation of *P.*

606 *judaica* to low Fe availability caused by high pH (Tric-treatment) and calcareous environment
607 (Bic). Indeed, the root architecture of the -Fe and Tric-treated plants was characterized by
608 the development of adventitious roots and branching zone associated with lower TD of
609 their root axes. In particular, the low TD of the root axes observed in Fe-deficient and Tric
610 treatments was negatively correlated with root exudation which, in turn, is a fundamental
611 physiological trait of the Fe deficiency syndrome (Ladygina and Hedlund, 2010; Hell and
612 Stephan, 2003; de Vries et al., 2019). This root trait, in association with a high aLA and
613 RBZ, explained the higher fitness of *P. judaica* plants as shown by Pearson correlations.
614 Conversely to the -Fe and Tric-treated plants, the root architecture of the Bic-treated ones was
615 characterized by higher LI but less TD. The Bic- induced calcareous environment affected the
616 availability of different nutrients, including P, Mn, B, and Zn (Tyler, 2003). In this study, a low
617 P content in roots and an Fe accumulation in the root apoplast was observed in Bic-treated
618 plants. In such conditions, the soil exploration by roots might be a strategy to survive in
619 calcareous soils (White et al., 2013; Campestre et al., 2016; Ding et al., 2019). Indeed, *P.*
620 *judaica* exposed to the calcareous condition displayed higher variability of root plasticity
621 with respect to plants exposed to the other treatments, by reducing the branching zone,
622 increasing the branching density and lateral spread.
623 Direct (-Fe) as well as induced Fe deficiency (Bic, Tric), all caused an increase in caffeoylquinic
624 acid derivatives, especially in Bic-treated roots (both tissues and exudates). Interestingly,
625 caffeic acid, probably arising from hydrolysis of caffeoylquinic esters, is one of the components
626 of the root exudates. The accumulation of phenolics in plant tissues is a hallmark of plant
627 stress: phenolic compounds may be synthesized *de novo* in plants as a response to various
628 biotic and abiotic stresses, including nutrient deficiency (Osmond et al., 1987; Cheynier et
629 al., 2013; Lattanzio, 2019). Several studies have reported the increase in chlorogenic acid
630 and/or mono- and di-caffeoylquinic acid in response to different abiotic stresses such as
631 low-temperature (Lattanzio and Van Sumere, 1987; Lattanzio et al., 2001; Lattanzio et al.,
632 1994), wounding (Cantos et al., 2001), high UV-B irradiation and insect attack (Izaguirre
633 et al., 2007).
634 Caffeoylquinic acid (CQA) derivatives are caffeic acid (3,4-dihy- droxycinnamic acid)
635 depsides, positional isomers of caffeic acid esters of quinic acid, which are broadly distributed
636 in plants. The chelating activity of CQAs is attributed to their catechol ring (Kono et al., 1998).
637 Low temperature stress induces, in artichoke tissues, an accumulation of constitutive
638 phenolic compounds, mono- and di-caffeoylquinic acids, that protect chilled tissues from
639 damage by free radical-induced oxidative stress (Lattanzio et al., 1994). Due to the presence
640 of a catechol ring in its structure, chlorogenic acid can promote the reductive release of

ferritin Fe as mobile Fe^{2+} that, in turn, forms colourless complexes with the excess of chlorogenic acid (Boyer et al., 1988). Hence, chlorogenic acid can act as a reductant of Fe^{3+} as well as a ligand of Fe^{2+}. In addition, this paper shows that the exudation process produces, likely by hydrolytic processes, caffeic acid, which has a high Fe reduction ability. Overall, the results in the present work support the current view that secretion of phenolic compounds is a relevant component of the reduction strategy of Fe acquisition in non-graminaceous plants. In the past decades, several studies suggested that the secreted phenolics could enhance Fe availability in the rhizosphere soil, as an alternative/reinforcement of the membrane-bound reductase, through chelation and reduction of insoluble Fe. Initially, phenolics were thought to help with the solubilization and reutilization of apoplastic Fe in red clover. This feature was not considered part of the Fe uptake mechanism until coumarin derived phenolics were observed in *Arabidopsis* under high pH conditions (Fourcroy et al., 2014). Other plant species such as peanut (*Arachis hypogaea* L.) and rice (*Oryza sativa*) plants secrete other phenylpropanoids instead of coumarins, which also facilitate the reduction of ferric Fe (Romheld and Marschner, 1983; Ishimaru et al., 2011).

Root exudates collection was performed using a hydroponic-only system which is useful for the characterization of specific compounds, avoiding alteration via sorption processes to the soil matrix and microbial decomposition (Oburger and Jones, 2018). However, soil-specific resource availability and microbiome activity are important factors affecting plant metabolism and root exudation, and therefore hydroponic-only systems are less suitable to provide useful information about the metabolites released by roots (Oburger and Jones, 2018). Nevertheless, by setting up different treatments mimicking an alkaline or calcareous conditions, our approach allowed us to identify differential phenolics exudation patterns in direct (-Fe) and induced Fe deficiency (Bic and Tric) conditions. However, further analyses are required to provide more details on the root exudation from *P. judaica*. In addition, it has been suggested that the root Fe deficiency response also includes the dynamic use of a large Fe reservoir bound to cell wall components in the root apoplast, secretion of phenolic compounds in the apoplast, and inhibition of suberization of endodermal cells in order to allow apoplastic and transcellular radial transport of Fe (Romheld and Marschner, 1983; Jin et al., 2007, 2008; Ishimaru et al., 2011; Connorton et al., 2017). Accordingly, the increased cell wall lignification, together with the high apoplastic Fe accumulation observed in Bic-treated roots, are in agreement with these findings. Recently, it has been suggested that kiwifruit plants activate two different

675 strategies to acquire and translocate Fe from the –Fe or + Bic nutrient solution (Wang et al.,
676 2020). Under -Fe conditions, a foraging-reusing strategy increased the mobilization of Fe
677 (by the release of hemicellulose Fe from the cell wall and the redistribution of water-soluble
678 Fe and apoplastic Fe in roots). However, under + Bic conditions, roots employed a
679 resisting-inactivating strategy due to the bicarbonate-mediated inhibition of Fe
680 translocation from root to shoot, resulting in an accumulation of water-soluble and
681 apoplastic Fe and slowing down the release of hemicellulose Fe in the cell wall (Wang et
682 al., 2020).
683 The approach employed highlighted several differences between direct (-Fe) and induced
684 Fe deficiency (Bic and Tric) treatments. Other than the presence of bicarbonate, such
685 differences are also attributable to the high pH. Recently it has been demonstrated that the
686 environ- mental pH is an important determinant of global gene expression which tunes Fe
687 acquisition to the prevailing edaphic conditions in Arabidopsis plants. Under high pH, Fe
688 deficiency responses are affected, and the production and secretion of Fe-mobilizing
689 coumarins is induced, prioritizing the most effective strategy to mobilize Fe from otherwise
690 inaccessible pools. Furthermore, at transcriptional level, Fe-deficient plants grown at high
691 pH displayed an increased expression of genes involved in the orchestration of defence
692 responses to pathogens (Tsai, 2020).
693 Furthermore, the exudation of phenolics into the rhizosphere in- fluences selectively some
694 microbial soil species that produce either siderophores or auxins that support Fe
695 acquisition by the plant (Jin et al., 2008; Stringlis et al., 2018). The overall microbiome
696 associated with the roots of *P. judaica* differed from that of the bulk soil, indicating that
697 plants in urban soil carry out microbial recruitment. The coumarin mechanism for shaping
698 root-associated microbioma is mainly associated to the catechol moiety of such compounds,
699 which can mobilize Fe and produce ROS, playing a detrimental effect on the growth of
700 some microbial genera (Voges et al., 2019). A mechanism similar to that suggested for
701 coumarins in the rhizosphere might also occur for *P. judaica* phenolics, as they also display
702 both the catechol moiety in their chemical structures and Fe reducing activity.
703
704 **Funding**
705 This work was supported by the local research funds of the Depart- ment of Life Science and
706 Systems Biology, University of Turin.
707
708 **Authorship**

All the authors have made substantial contributions to conception and design, or acquisition of data, or analysis and interpretation of data (G.V, G.Z, I.M, conception and design; LT, plant growth, exudate collection, organic acid analysis; E.E, M.N, A.S, microbiome characterization and data elaboration; V.La, V.Li phenols characterization; M.A, A.S, root architecture analysis; M.D, histological analysis; G.V., S.A., soil analysis and plant nutrient analysis); G.V and I.M. drafted the manuscript. All the authors participate in revising the manuscript.

Declaration of competing interest

The authors declare that they have no known competing financial interests or personal relationships that could have appeared to influence the work reported in this paper.

Acknowledgements

We thank Dr. Veronica Lattanzio for supporting HPLC-MS analysis.

References

Abenavoli, M.R., Sorgonà, A., Albano, S., Cacco, G., 2004. Coumarin differentially affects the morphology of different root types of maize seedlings. J. Chem. Ecol. 30 (9), 1871–1883.

Abenavoli, M.R., Nicolo`, A., Lupini, A., Oliva, S., Sorgonà, A., 2008. Effects of different allelochemicals on root morphology of *Arabidopsis thaliana*. Allelopathy J. 22, 245–252.

Abenavoli, M.R., Leone, M., Sunseri, F., Bacchi, M., Sorgona`, A., 2016. Root phenotyping for drought tolerance in bean landraces from Calabria (Italy). J. Agron. Crop Sci. 202 (1), 1–12. https://doi.org/10.1111/jac.1212.

Atkinson, J.A., Rasmussen, A., Traini, R., Voß, U., Sturrock, C., Mooney, S.J., Wells Darren, M., Bennett, M.J., 2014. Branching out in roots: uncovering form, function, and regulation. Plant Physiol. 166 (2), 538–550. https://doi.org/10.1104/pp.114.245423.

Badri, D.V., Chaparro, J.M., Zhang, R., Shen, Q., Vivanco, J.M., 2013. Application of natural blends of phytochemicals derived from the root exudates of Arabidopsis to the soil reveal that phenolic-related compounds predominantly modulate the soil microbiome. J. Biol. Chem. 15 (7), 4502–4512. https://doi.org/10.1074/jbc.M112.433300, 288.

744 Barberon, M., Vermeer, J.E., De Bellis, D., Wang, P., Naseer, S., Andersen, T.G.,
745 Humbel, B.M., Nawrath, C., Takano, J., Salt, D.E., Geldner, N., 2016. Adaptation of
746 root function by nutrient-induced plasticity of endodermal differentiation. Cell 164 (3),
747 447–459.
748 Bartoli, G., Bottega, S., Forino, L.M.C., Ruffini Castiglione, M., Tagliasacchi, A.M.,
749 Grilli, I., Spano`, C., 2013. Morpho-physiological plasticity contributes to tolerance of
750 *Calluna vulgaris* in an active geothermical field. Austr. J. Botany 61, 107–118.
751 Bechtold, U., 2018. Plant life in extreme environments: how do you improve
752 drought tolerance? Front. Plant Sci. 9, 543.
753 https://doi.org/10.3389/fpls.2018.00543.
754 Bolyen, E., Rideout, J.R., Dillon, M.R., Bokulich, N.A., Abnet, C.C., Al-Ghalith, G.A.,
755 Alexander, H., Knight, R., Caporaso, J.G., 2019. Reproducible, interactive, scalable
756 and extensible microbiome data science using QIIME 2. Nat. Biotechnol. 37, 852–857.
757 https://doi.org/10.1038/s41587-019-0209-9.
758 Boyer, R.F., Clark, H.M., LaRoche, A.P., 1988. Reduction and release of ferritin iron
759 by plant phenolics. J. Inorg. Biochem. 32 (3), 171–181. https://doi.org/10.1016/0162-
760 0134(88)80025-4. PMID: 3131480.
761 Bulgarelli, D., Rott, M., Schlaeppi, K., Ver Loren van Themaat, E., Ahmadinejad, N.,
762 Assenza, F., Rauf, P., Huettel, B., Reinhardt, R., Schmelzer, E., 2012. Revealing
763 structure and assembly cues for Arabidopsis root-inhabiting bacterial microbiota.
764 Nature 488, 91–95.
765 Campestre, M.P., Antonelli, C., Calzadilla, P.I., Maiale, S.J., Rodríguez, A.A., Ruiz,
766 O.A., 2016. The alkaline tolerance in *Lotus japonicus* is associated with mechanisms
767 of iron acquisition and modification of the architectural pattern of the root. J. *Plant*
768 *Physiol.* 206, 40–48.
769 Cantos, E., Espin, J.C., Tomas-BarberanF, A., 2001. Effect of wounding on phenolic
770 enzymes in six minimally processed lettuce cultivars upon storage. J. Agric. Food
771 Chem. 49, 322–330.
772 Caporaso, J.G., Kuczynski, J., Stombaugh, J., Bittinger, K., Bushman, F.D., Costello,
773 E.K., et al., 2010. QIIME allows analysis of high-throughput community sequencing
774 data. Nat. Methods 7, 335–336.
775 Caretto, S., Linsalata, V., Colella, G., Mita, G., Lattanzio, V., 2015. Carbon fluxes
776 between primary metabolism and phenolic pathway in plant tissues under stress. Int.
777 J. Mol. Sci. 16 (11), 26378–26394. https://doi.org/10.3390/ijms161125967.
778 Cesco, S., Neumann, G., Tomasi, N., Pinton, R., Weisskopf, L., 2010. Release of plant-

779 borne flavonoids into the rhizosphere and their role in plant nutrition. Plant Soil 329
780 (1–2), 1–25.
781 Chaney, R.L., Brown, J.C., Tiffin, L.O., 1972. Obligatory reduction of ferric chelates
782 in iron uptake by soybeans. Plant Physiol. 50, 208–213.
783 Chen, Y., Barak, P., 1982. Iron nutrition of plants in calcareous soils. Adv. Agron. 35,
784 217–240.
785 Chen, J., Bittinger, K., Charlson, E.S., Hoffmann, C., Lewis, J., Wu, G.D., Collman,
786 R.G., Bushman, F.D., Li, H., 2012. Associating microbiome composition with
787 environmental covariates using generalised UniFrac distances. Bioinformatics 28 (16),
788 2106–2113.
789 Cheynier, V., Comte, G., Davies, K.M., Lattanzio, V., Martens, S., 2013. Plant
790 Phenolics: recent advances on their biosynthesis, genetics, and ecophysiology. Plant
791 Physiol. Biochem. 72, 1–20.
792 Ciamporova, M., Dekankova, K., Ovecka, M., 1998. Intra- and interspecific variation
793 in root length, root turnover and the underlying parameters. In: Lambers, H., Poorter,
794 H., VanVuuren, M.M.I. (Eds.), Variation in Plant Growth. *Physiological Mechanisms*
795 *and Ecological Consequences*. Backhuys Publishers, Leiden, pp. 57–69.
796 Coleman, J.S., McConnaughay, K.D.M., Ackerly, D.D., 1994. Interpreting phenotypic
797 variation in plants. Trends Ecol. Evol. 9, 187–191.
798 Connorton, J.M., Balk, J., Rodríguez-Celma, J., 2017. Iron homeostasis in plants – a
799 brief overview. Metall 9, 813–823.
800 Csardi, G., Nepusz, T., 2006. The igraph software package for complex network
801 research. Inter J. Complex Syst. 1695. http://igraph.org.
802 de Vries, F.T., Williams, A., Stringer, F., Willcocks, R., McEwing, R., Langridge,
803 H., Straathof, A.L., 2019. Changes in root-exudate-induced respiration reveal a
804 novel mechanism through which drought affects ecosystem carbon cycling. New
805 Phytol. 224 (1), 132–145. https://doi.org/10.1111/nph.16001.
806 Dell'Orto, M., De Nisi, P., Pontiggia, A., Zocchi, G., 2003. Fe Deficiency Responses in
807 *Parietaria diffusa*: a calcicole plant. J. Plant Nutr. 26 (10–11), 2057–2068.
808 Díaz, I., Delgado, A., de Santiago, A., del Campillo, M.C., Torrent, J., 2012. Iron
809 deficiency chlorosis in plants as related to Fe sources in soil. EGU General Assem. 22–
810 27 April, 4454, 2012, Vienna-Austria.
811 Ding, W., Clode, P.L., Lambers, H., 2019. Is pH the key reason why some *Lupinus*
812 species are sensitive to calcareous soil? Plant Soil 434, 185–201.
813 https://doi.org/10.1007/ s11104-018-3763-x.

814 Donnini, S., Castagna, A., Ranieri, A., Zocchi, G., 2009. Differential responses in pear
815 and quince genotypes induced by Fe deficiency and bicarbonate. J. Plant Physiol. 166,
816 1181–1193.
817 Donnini, S., Dell'Orto, M., Zocchi, G., 2011. Oxidative stress responses and root
818 lignification induced by Fe deficiency conditions in pear and quince genotype. Tree
819 Physiol. 31, 102–113.
820 Donnini, S., De Nisi, P., Gabotti, D., Tato, L., Zocch, iG., 2012. Adaptive strategies of
821 *Parietaria diffusa* (M.&K.) to calcareous habitat with limited iron availability. Plant
822 Cell Environ. 35 (6), 1171–1184.
823 Dubrovsky, J.G., Forde, B.G., 2012. Quantitative analysis of lateral root
824 development: pitfalls and how to avoid them. Plant Cell 24 (1), 4–14.
825 https://doi.org/10.1105/ tpc.111.089698.
826 Edgar, R.C., Haas, B.J., Clemente, J.C., Quince, C., Knight, R., 2011. UCHIME
827 improves sensitivity and speed of chimera detection. Bioinformatics 27 (16), 2194–
828 2200.
829 Edwards, J., Johnson, C., Santos-Medellín, C., Lurie, E., Podishetty, N.K., Bhatnagar,
830 S., Eisen, J.A., Sundaresan, V., 2015. Structure, variation, and assembly of the root-
831 associated microbiomes of rice. Proc. Natl. Acad. Sci. U.S.A. 24 (8), E911–E920.
832 https://doi.org/10.1073/pnas.1414592112, 112.
833 Faria, J.C., Jelihovschi, E.G., Allaman Bezerra, I., 2016. Conventional Tukey Test.
834 UESC, Ilheus, Brasil.
835 Fourcroy, P., Sisò-Terraza, P., Sudre, D., Saviro´n, M., Reyt, G., Gaymard, F., Abadía,
836 A., Abadia, J., Alvarez-Fern´andez, A., Briat, J.F., 2014. Involvement of the ABCG37
837 transporter in secretion of scopoletin and derivatives by Arabidopsis roots in response
838 to iron deficiency. New Phytol. 201, 155–167.
839 Harbort, C.J., Hashimoto, M., Inoue, H., Niu, Y., Guan, R., Rombola`, A.D., Kopriva,
840 S., Voges, M.J.E.E.E., Sattely, E.S., Garrido-Oter, R., Schulze-Lefert, P., 2020. Root-
841 secreted coumarins and the microbiota interact to improve iron nutrition in
842 Arabidopsis. Dec 9 Cell Host Microbe 28 (6), 825–837. https://doi.org/10.1016/j.
843 chom.2020.09.006. e6.
844 Hartman, K., van der Heijden, M.G.A., Wittwer, R.A., et al., 2018. Cropping
845 practices manipulate abundance patterns of root and soil microbiome members
846 paving the way to smart farming. Microbiome 6, 14.
847 https://doi.org/10.1186/s40168-017- 0389-9.
848 Hell, R., Stephan, U.W., 2003. Iron uptake, trafficking and homeostasis in plants.

Planta 216, 541–551.
Henkhaus, N., Barlett, M., Gang, D., Grumet, R., Jordan-Thaden, I., Lerence, A., Lyons, E., Miller, S., et al., 2020. Plant Science decadal vision 2020-2030: reimagining the potential of plants for a healthy and sustainable future. Plant Direct 1–24. https://doi.org/10.1002/pld3.252, 00.
Ho, M.D., Rosas, J.C., Brown, K.M., Lynch, J.P., 2005. Root architectural tradeoffs for water and phosphorus acquisition. Funct. Plant Biol. 32, 737–748.
Hu, H., Tang, C., Rengel, Z., 2005. Influence of phenolic acids on phosphorus mobilization in acidic and calcareous soils. Plant Soil 268, 173–180.
Hummel, I., Vile, D., Violle, C., Devaux, J., Ricci, B., Blanchard, A., Garnier, E., Roumet, C., 2007. Relating root structure and anatomy to whole-plant functioning in 14 herbaceous Mediterranean species. New Phytol. 173 (2), 313–321.
Ihrmark, K., Bo¨deker, I.T.M., Cruz-Martinez, K., Friberg, H., Kubartova, A., Schenck, J., Strid, Y., Stenlid, J., Brandstro¨m-Durling, M., Clemmensen, K.E., Lindahl, B.D., 2012. New primers to amplify the fungal ITS2 region – evaluation by 454-sequencing of artificial and natural communities. FEMS (Fed. Eur. Microbiol. Soc.) Microbiol. Ecol. 82 (3), 666–677.
Isah, T., 2019. Stress and defense responses in plant secondary metabolites production. Biol. Res. 52, 1–25.
Ishimaru, Y., Kakei, Y., Shimo, H., Bashir, K., Sato, Y., Sato, Y., Uozumi, N., Nakanishi, H., Nishizawa, N.K., 2011. A rice phenolic efflux transporter is essential for solubilizing precipitated apoplasmic iron in the plant stele. J. Biol. Chem. 286 (28), 24649–24655.
Izaguirre, M.M., Mazza, C.A., Svatos, A., Baldwin, I.T., Ballare, C.L., 2007. Solar ultraviolet-B radiation and insect herbivory trigger partially overlapping phenolic responses in Nicotiana attenuate and Nicotiana longiflora. Ann. Bot. 99, 103–109.
Jansenn, P.H., 2006. Identifying the Dominant Soil Bacterial Taxa in Libraries of 16S rRNA and 16S rRNA Genes Applied and Environmental Microbiology, vol. 72. https://doi.org/10.1128/AEM.72.3.1719-1728.2006, 3.
Jin, C.W., You, G.Y., He, Y.F., Tang, C.X., Wu, P., Zheng, S.J., 2007. Iron deficiency-induced secretion of phenolics facilitates the reutilization of root apo-plastic iron in red clover. Plant Physiol. 144, 278–285.
Jin, C.W., You, G.Y., Zheng, S.J., 2008. The iron deficiency-induced phenolics secretion plays multiple important roles in plant iron acquisition underground. Plant Signal. Behav. 3 (1), 60–61.

884 Kalayu, G., 2019. Posphorus solubilising microorganisms: promising approach as
885 biofertilizers. Int. J. Agron. https://doi.org/10.1155/2019/4917256. ID 4917256.
886 Kim, S.A., Guerinot, M.L., 2007. Mining iron: iron uptake and transport in plants.
887 FEBS Lett. 581 (12), 2273–2280.
888 Kobayashi, T., Nishizawa, N.K., 2012. Iron uptake, translocation, and regulation in
889 higher plants. Annu. Rev. Plant Biol. 63, 131–152.
890 Kono, Y., Kashine, S., Yoneyama, T., Sakamoto, Y., Matsui, Y., Shibata, H., 1998.
891 Iron chelation by chlorogenic acid as a natural antioxidant. Biosci. Biotechnol.
892 Biochem. 62 (1), 22–27. https://doi.org/10.1271/bbb.62.22. PMID: 9501514.
893 Ladygina, N., Hedlund, K., 2010. Plant species influence microbial diversity and
894 carbon allocation in the rhizosphere. Soil Biol. Biochem. 42, 162–168.
895 Lattanzio, V., 2019. Relationship of phenolic metabolism to growth in plant and cell
896 cultures under stress. In: Ramawat, K.G., Ekiert, H.M., Goyal, S. (Eds.), Plant Cell and
897 Tissue Differentiation and Secondary Metabolites, Reference Series in
898 Phytochemistry. Springer Nature Switzerland AG, pp. 1–32.
899 Lattanzio, V., Van Sumere, C.F., 1987. Changes in phenolic compounds during the
900 development and cold storage of artichoke (Cynara scolymus L. heads). Food Chem.
901 24 (1), 37.
902 Lattanzio, V., Cardinali, A., Di Venere, D., Linsalata, V., Palmieri, S., 1994. Browning
903 phenomena in stored artichoke (*Cynara scolymus* L.) heads: enzymic or chemical
904 reactions? Food Chem. 50, 1–7.
905 Lattanzio, V., Di Venere, D., Linsalata, V., Bertolini, P., Ippolito, A., Salerno, M.,
906 2001. Low temperature metabolism of apple phenolics and quiescence of *Phlyctanea*
907 *vagabunda*. J. Agric. Food Chem. 49 (12), 5817–5821.
908 Lindsay, W.L., Schwab, A.P., 1982. The chemistry of iron in soils and its availability
909 to plants. J. Plant Nutr. 5, 821–840.
910 Lupini, A., Sorgonà, A., Princi, M.P., Sunseri, F., Abenavoli, M.R., 2016.
911 Morphological and physiological effects of trans-cinnamic acid and its hydroxylated
912 derivatives on maize root types. Plant Growth Regul. 78 (2), 263–273.
913 https://doi.org/10.1007/ s10725-015-0091-5.
914 McMurdie, P.J., Holmes, S., 2013. Phyloseq: an R package for reproducible interactive
915 analysis and graphics of microbiome census data. PLoS One 8 (4), e61217.
916 Mehboob, I., Naveed, M., Zahir, Z.A., Ashraf, M., 2012. Potential of Rhizobia for
917 sustainable production of non-legumes. In: Ashraf, M., Oztürk, M., Ahmad, M.,
918 Aksoy, A. (Eds.), Crop Production for Agricultural Improvement. Springer,

Dordrecht. https://doi.org/10.1007/978-94-007-4116-4_26.
Mengel, K., 1994. Iron availability in plant tissues—iron chlorosis on calcareous soils. Plant Soil 165, 275–283.
Miguel, M.A., Postma, J.A., Lynch, J.P., 2015. Phene synergism between root hair length and basal root growth angle for phosphorus acquisition. Plant Physiol. 167 (4), 1430–1439. https://doi.org/10.1104/pp.15.00145.
Mimmo, T., Ghizzi, M., Marzadori, C., et al., 2008. Organic acid extraction from rhizosphere soil: effect of field-moist, dried and frozen samples. Plant Soil 312, 175–184. https://doi.org/10.1007/s11104-008-9574-8.
Oburger, E., Jones, D.L., 2018. Sampling root exudates-mission impossible? Rhizosphere 6 (2018), 116–133.
Oksanen, J., Blanchet, F.G., Kindt, R., Legendre, P., Minchin, P.R., O'Hara, R.B., Simpson, G.L., Solymos, P., Stevens, M.H.H., Wagner, H., 2013. Vegan: community ecology package [WWW document] URL. http://cran.r-project.org/package=vegan.
Osmond, C.B., Austin, M.P., Berry, J.A., Billings, W.D., Boyer, J.S., Dacey, J.W.H., Nobel, P.S., Smith, S.D., Winner, W.E., 1987. Stress physiology and the distributions of plants. Bioscience 37, 38–48.
Pedregosa, F., Varoquaux, G., Gramfort, A., Michel, V., Thirion, B., Grisel, O., Blondel, M., Prettenhofer, P., Weiss, R., Dubourg, V., Vanderplas, J., Passos, A., Cournapeau, D., Brucher, M., Perrot, M., Duchesnay, E., 2011. Scikit-learn: machine learning in Python. J. Mach. Learn. Res. 12, 2825–2830.
Perez-Jaramillo, J.E., Mendes, R., Raaijmakers, J.M., 2016. Impact of plant domestication on rhizosphere microbiome assembly and functions. Plant Mol. Biol. 90 (6), 635–644. https://doi.org/10.1007/s11103-015-0337-7.
Quast, C., Pruesse, E., Yilmaz, P., Gerken, J., Schweer, T., Yarza, P., et al., 2012. The SILVA ribosomal RNA gene database project: improved data processing and web-based tools. Nucleids Acids Res. 41, 590–596.
Rajniak, J., Giehl, R.F., Chang, E., Murgiam, I., von Wiren, N., Sattely, E.S., 2018. Biosynthesis of redox-active metabolites as a general strategy for iron acquisition in plants. Nat. Chem. Biol. 442, 450. https://doi.org/10.1038/s41589-018-0019-2.
Rangarajan, H., Postma, J.A., Lynch, J.P., 2018. Co-optimisation of axial root phenotypes for nitrogen and phosphorus acquisition in common bean. Ann. Bot. 122, 485–499. https://doi.org/10.1093/aob/mcy092.
Ranjani, A., Dhanasekaran, D., Gopinath, P.M., 2016. An Introduction to

Actinobacteria. https://doi.org/10.5772/62329, 11th 2016.
Roman-Aviles, B., Snapp, S.S., Kelly, J.D., 2004. Assessing root traits associated with root rot resistance in common bean. Field Crop. Res. 86, 147–156.
Romano, A., Sorgonà, A., Lupini, A., Araniti, F., Stevanato, P., Cacco, G., Abenavoli, M. R., 2013. Morpho-physiological responses of sugar beet (*Beta vulgaris* L.) genotypes to drought stress. Acta Physiol. Plant. 35, 853–865. https://doi.org/10.1007/ s11738-012-1129-1.
Romheld, V., 1987. Different strategies for iron acquisition in higher plants. Physiol. Plantarum 70 (2), 231–234.
Romheld, V., Marschner, H., 1983. Mechanism of iron uptake by peanut plants. I. Fe"' reduction, chelate splitting, and release of phenolics. Plant Physiol. 71, 949–955.
Ryser, P., Lambers, H., 1995. Root and leaf attributes accounting for the performance of fast- and slow-growing grasses at different nutrient supply. Plant Soil 170, 251–265.
Sasse, J., Martinoia, E., Northen, T., 2018. Feed your friends: do plant exudates shape the root microbiome? Trends Plant Sci. 23 (1), 25–41. https://doi.org/10.1016/j.tplants.2017.09.003. Epub 2017 Oct 17. PMID: 29050989.
Sathya, A., Rajendran Vijayabharathi, R., Gopalakrishnan, S., 2017. Plant growth-promoting actinobacteria: a new strategy for enhancing sustainable production and protection of grain legumes. Biotechnology 7 (2), 102. https://doi.org/10.1007/ s13205-017-0736-3.
Schenkeveld, W.D.C., Kraemer, S.M., 2018. Constraints to synergistic Fe mobilization from calcareous soil by a phytosiderophore and a reductant. Soil Systems 4, 67. https://doi.org/10.3390/soilsystems2040067.
Sorgona`, A., Abenavoli, M.R., Gringeri, P.G., Cacco, G., 2007. Comparing morphological plasticity of root orders in slow- and fast-growing citrus rootstocks supplied with different nitrate levels. Ann. Bot. 100, 1287–1296. https://doi.org/10.1093/aob/ mcm207.
Stevanato, S., Gui, G., Cacco, G., Biancardi, E., Abenavoli, M.R., Romano, A., Sorgonà, A., 2013. Morpho-physiological traits of sugar beet exposed to salt stress. Int. Sugar J. 115, 800–809.
Stringlis, I.A., Yu, K., Feussner, K., de Jonge, R., Van Betum, S.V., Van Vek, M.C., Berendsen, R.L., Bakker, P.A.H.M., Feussner, I., Pieterse, C.M.J., 2018. MYB2-dependent coumarin exudation shapes root microbiome assembly to promote plant health. Proc. Natl. Acad. Sci. Unit. States Am. 115, E5213–E5222.
Takahashi, S., Tomita, J., Nishioka, K., Hisada, T., Nishijima, M., 2014. Development

of a prokaryotic universal primer for simultaneous analysis of Bacteria and Archaea using next-generation sequencing. PLoS One 9 (8), e105592.

Tato, L., De Nisi, P., Donnini, S., Zocchi, G., 2013. Low iron availability and phenolic metabolism in a wild plant species (*Parietaria judaica* L.). Plant Physiol. Biochem. 72, 145–153. https://doi.org/10.1016/j.plaphy.2013.05.017.

Tato, L., Islam, M., Mimmo, T., Zocchi, G., Vigani, G., 2020. Temporal responses to direct and induced iron deficiency in *Parietaria judaica*. Agronomy 10, 1037. https://doi. org/10.3390/agronomy10071037.

Tedersoo, L., Bahram, M., Po˜lme, S., Ko˜ljalg, U., Yorou, N.S., Wijesundera, R., Villarreal- Ruiz, L., et al., 2014. Global diversity and geography of soil fungi. Science 346, 1078.

Tellah, S., Badiani, M., Trifilo`, P., Lo Gullo, M.A., Ounane, G., Ounane, S.M., Sorgonà, A., 2014. Morpho-physiological traits contributing to water stress tolerance in a peanut (Arachis hypogaea L.) landraces collection from the Algerian Maghreb. Agrochimica 58, 126–147.

Teres, J., Busoms, S., Perez Martín, L., et al., 2019. Soil carbonate drives local adaptation in Arabidopsis thaliana. Plant Cell Environ. 42, 2384–2398. https://doi.org/ 10.1111/pce.13567.

Tsai, Schmidt, 2020. pH-dependent transcriptional profile changes in iron-deficient Arabidopsis roots. BMC Genom. 21, 694. https://doi.org/10.1186/s12864-020-07116-6.

Tyler, G., 2003. Some ecophysiological and historical approaches to species richness and calcicole/calcifuge behaviour—contribution to a debate. Folia Geobot. 38, 419–428.

Vigani, G., Murgia, I., 2018. Iron-Requiring enzymes in the spotlight of oxygen. Trends Plant Sci. 23, 874–882. https://doi.org/10.1016/j.tplants.2018.07.005.

Vives-Peris, V., Lopez-Climent, M.F., Perez-Clemente, R.M., Gomez-Cadenas, A., 2020. Root involvement in plant responses to adverse environmental conditions. Agronomy 10 (7), 942. https://doi.org/10.3390/agronomy10070942.

Voges, M.J.E.E.E., Bai, Y., Schulze-Lefert, P., Sattely, E.S., 2019. Plant-derived coumarins shape the composition of an Arabidopsis synthetic root microbiome. Proc. Natl. Acad. Sci. Unit. States Am. 116, 12558–12565.

Wahl, S., Ryser, P., 2000. Root tissue structure is linked to ecological strategies of grasses. New Phytol. 148, 459–471.

Wang, N., Dong, X., Chen, Y., Ma, B., Yao, C., Ma, F., Liu, Z., 2020. Direct and

Bicabonate-induced iron deficiency differentially affect iron translocation in kiwifruit roots. Plants 9, 1578. https://doi.org/10.3390/plants9111578.

White, P.J., George, T.S., Dupuy, L.X., Karley, A.J., Valentine, T.A., Wiesel, L., Wishart, J., 2013. Root traits for infertile soils. Front. Plant Sci. 4, 193. https://doi.org/10.3389/fpls.2013.00193.

Yilmaz, P., Parfrey, L.W., Yarza, P., Gerken, J., Pruesse, E., Quast, C., et al., 2013. The SILVA and "all-species living tree project (LTP)" taxonomic frameworks. Nucleids Acids Res. 42, 643–648.

York, L.M., Nord, E.A., Lynch, J.P., 2013. Integration of root phenes for soil resource acquisition. Front. Plant Sci. 4, 355. https://doi.org/10.3389/fpls.2013.00355.

Zadworny, M., Eissenstat, D.M., 2011. Contrasting the morphology, anatomy and fungal colonization of new pioneer and fibrous roots. New Phytol. 190, 213–221. https:// doi.org/10.1111/j.1469-8137.2010.03598.x.

Zajc, J., Gunde-Cimerman, N., 2018. The genus wallemia-from contamination of food to health threat. May 21 Microorganisms 6 (2), 46. https://doi.org/10.3390/microorganisms6020046. PMID: 29883408; PMCID: PMC6027281.

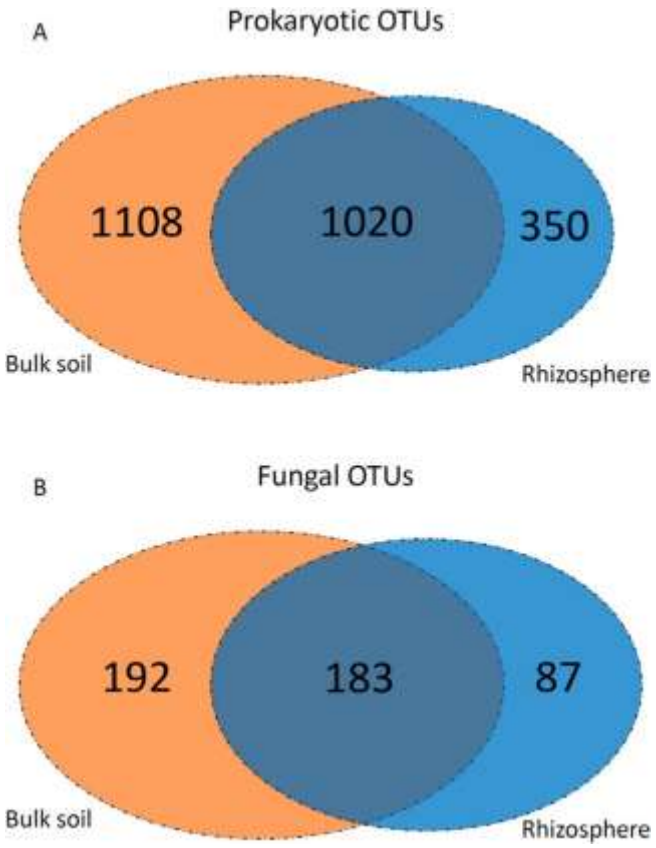

Fig. 1. Venn diagrams of the distribution of prokaryotic (A) and fungal (B) OTUs detected in bulk soil and rhizosphere samples. For each panel the number of identified OTUs in the bulk soil (in orange), and in the rhizosphere (in blue) are reported, as well as the number of overlapping OTUs. (For interpretation of the references to color in this figure legend, the reader is referred to the Web version of this article.)

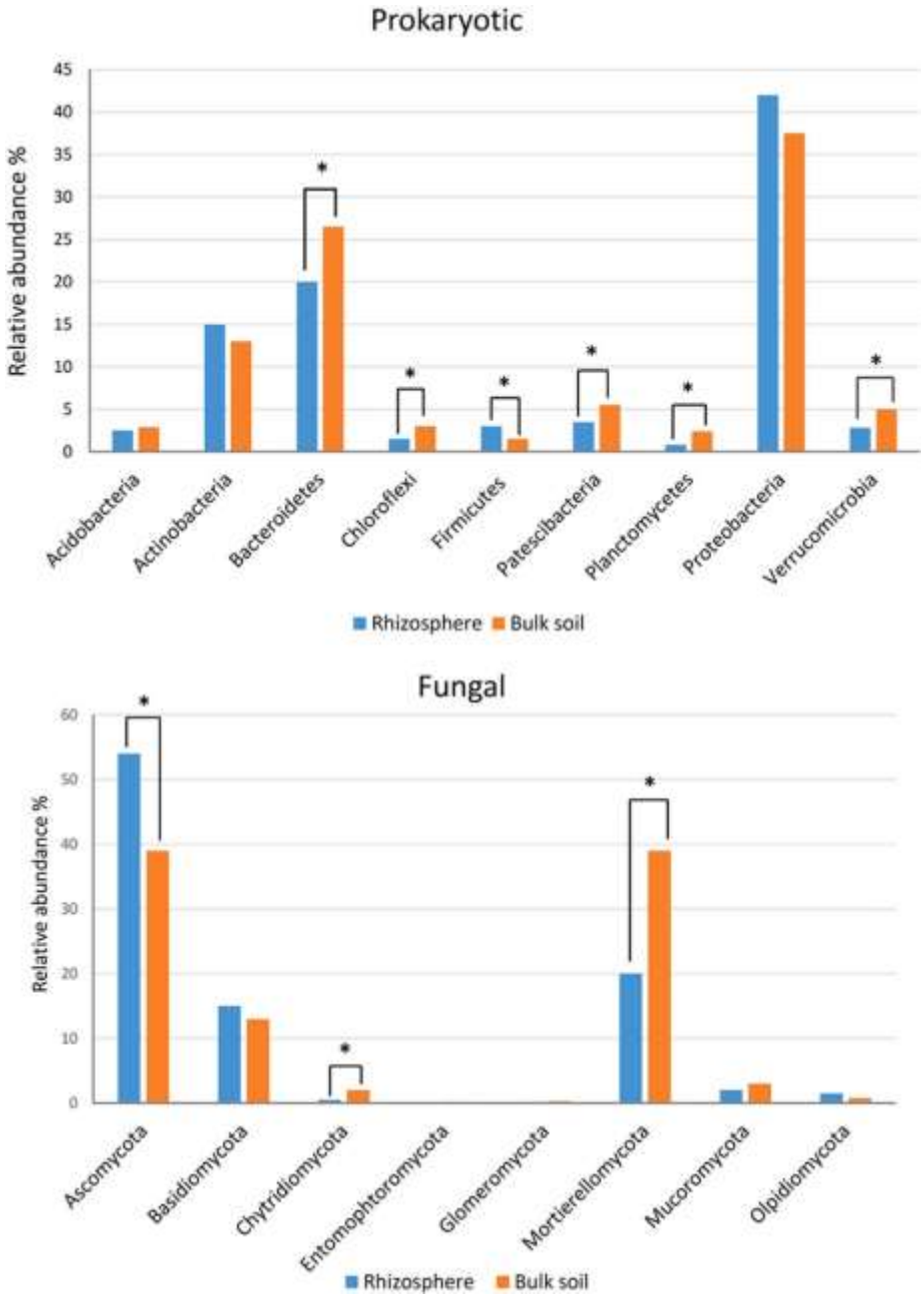

Fig. 2. Shifts in the microbial composition between the bulk soil and the rhizosphere microbiome at the phylum level. The bars show the relative abundance of each phylum on the overall microbial composition for the fungal (upper panel) and prokaryotic (lower panel) microbiome. Asterisks show significant differences in the bulk soil vs rhizosphere composition for each phylum displayed (p-value < 0.05). Eight independent biological replicates were considered ($n = 8$).

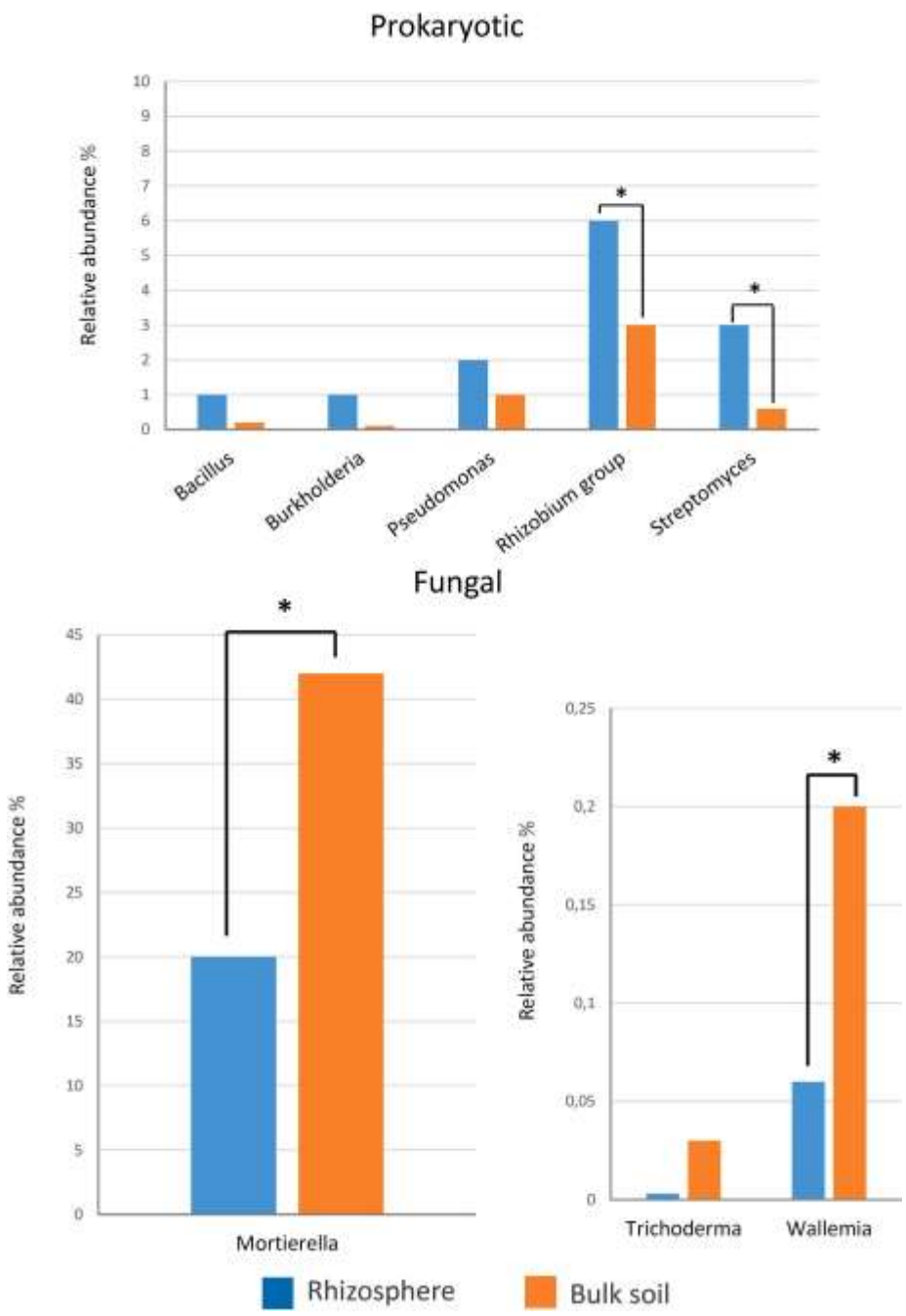

Fig. 3. Shifts in the microbial composition between the bulk soil and the rhizosphere microbiome at the genus level. The bars show the relative abundance on the overall microbial composition for the fungal and prokaryotic genera considered (n = 8). Asterisks show significant differences in the bulk soil vs rhizosphere composition for each genus displayed (p-value < 0.05). Note: the Rhizobium group comprises *Allorhizobium*, *Neorhizobium*, *Pararhizobium* and *Rhizobium*, as they are considered as a single genera according to the Silva taxonomy. Eight in- dependent biological replicates were considered (n= 8).

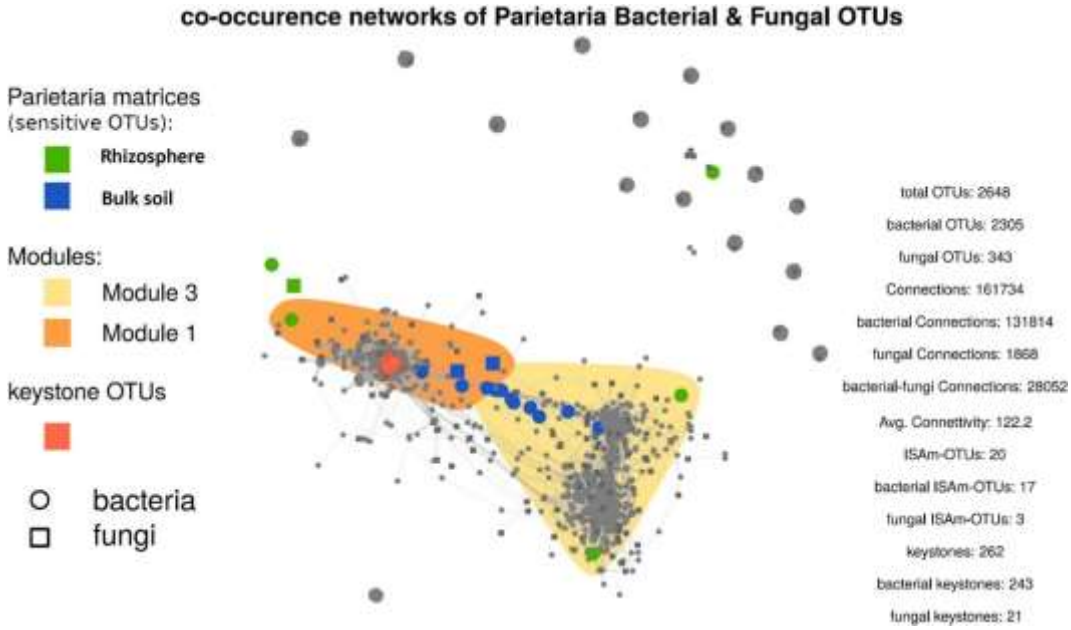

Fig. 4. Co-occurrence network (meta-network) visualising correlations between prokaryotic and fungal OTUs in the bulk soil and rhizosphere communities. The sensitive OTUs shown in green and blue represent the OTUs identified as indicator species for the rhizosphere and bulk soil condition, respectively (listed in supplemental file 3). Red triangles represent the Keystone OTUs (listed in supplemental file 2, red triangles) are also represented. Modules are defined as areas that show a high density of connections among OTUs. The Gray symbols represent "hot spots" of overlapping OTUs. (For interpretation of the references to color in this figure legend, the reader is referred to the Web version of this article.)

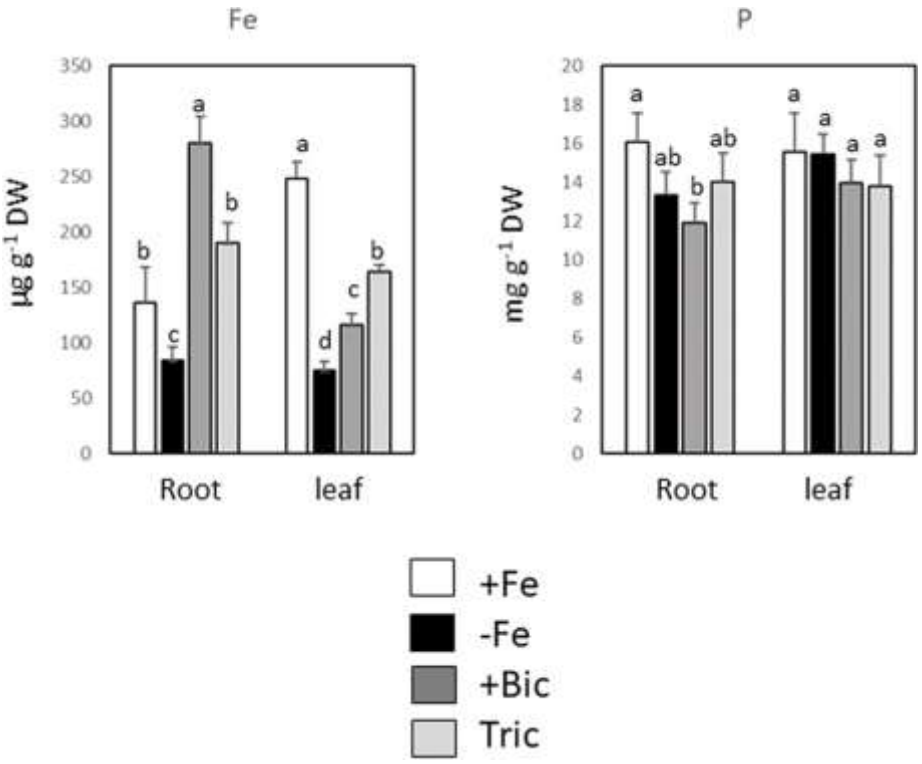

Fig. 5. Phosphorous (P) and iron (Fe) content in root and leaf tissues of *P. judaica* grown in +Fe, -Fe, Bic, and Tric treatments. Different letters correspond to significant differences among means ($P < 0.05$; Tukey test), $n = 3$.

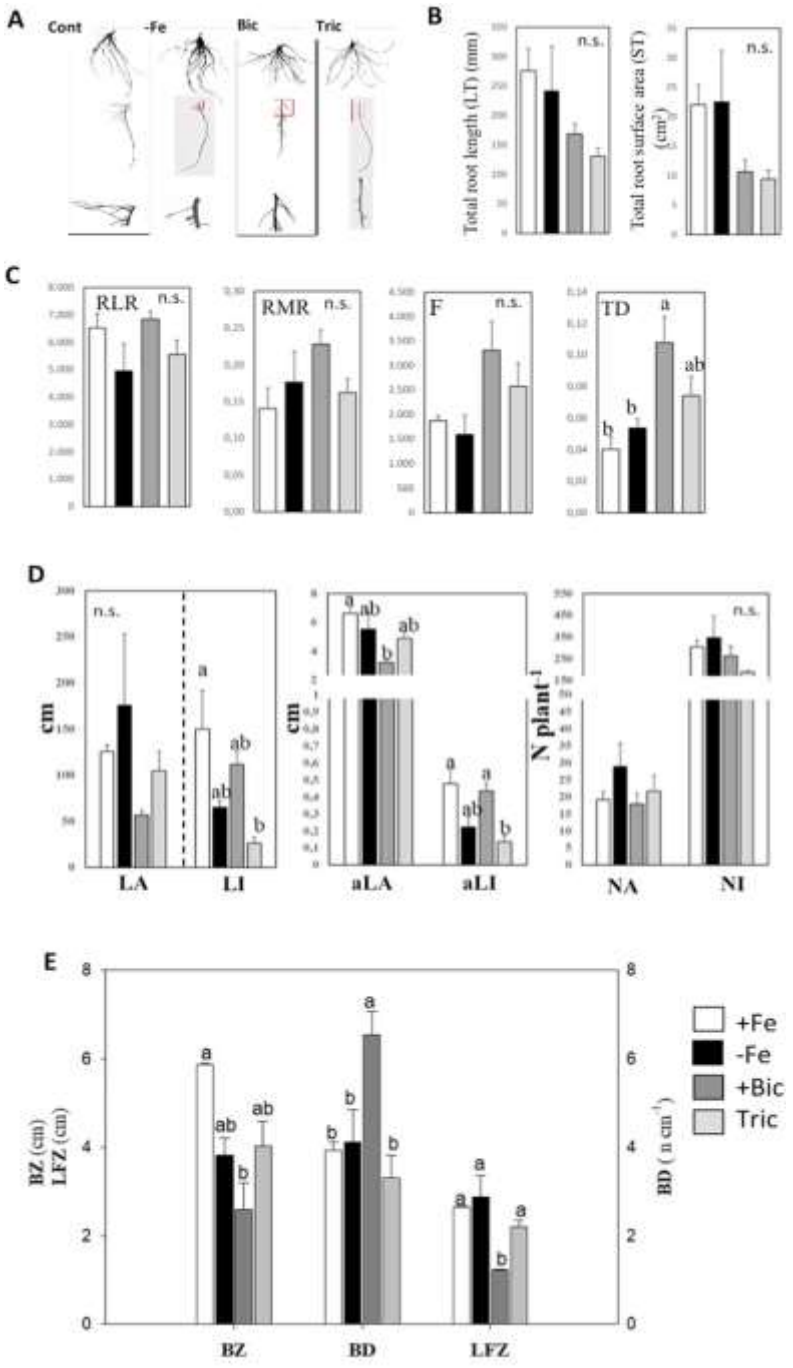

Fig. 6. Morphological analysis of the whole root system of *P. judaica* grown in +Fe, -Fe, Bic, and Tric media. A) Images captured of root; B) Total root length and total root surface; C) Root length ratio (RLR) and its components, i.e. root mass ratio RMR, fineness F and tissue density ratio TD; D) Morpho- logical analyses intra-root of lateral roots (LI, length; aLI, average length, NI, number) and adventitious roots (LA, length; aLA, average length, NA, number) (abbreviation are also reported in Table S1); E) Root branching analysis of *P. judaica* (root branching zone's length (BZ), lateral root formation zone (LRFZ)). Different letters correspond to statistically significant differences among mean values ($P < 0.05$; Tukey test), $n = 3$.

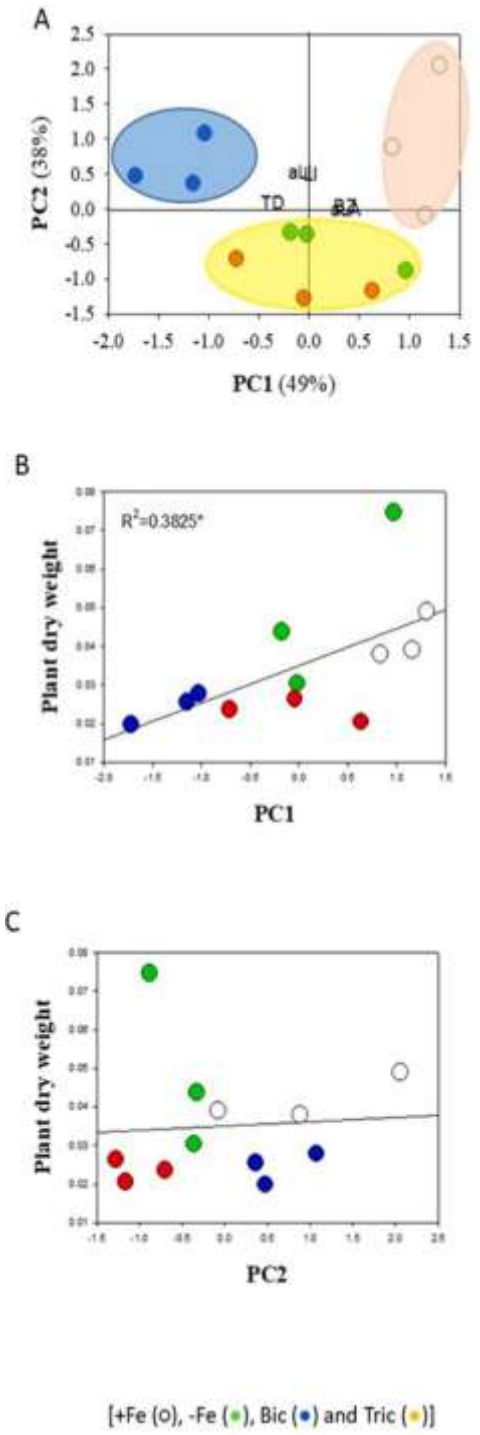

Fig. 7. A) Score and loading plots of principal component analysis of root traits from *P. judaica* plants exposed to + Fe, -Fe, Bic and Tric treatments. The proportion of variability explained by each PC is given within the bracket. The ellipses denote the grouping of the samples after Hierarchical Cluster Analysis (Ward's method with distance measure by squared Euclidean distance). Cor- relation between plant dry weight and PC1 (B) and PC2 (C) in *P. judaica* plants exposed to different treatments (+Fe, -Fe, Bic and Tric). The coefficient of determination and p-values are reported.

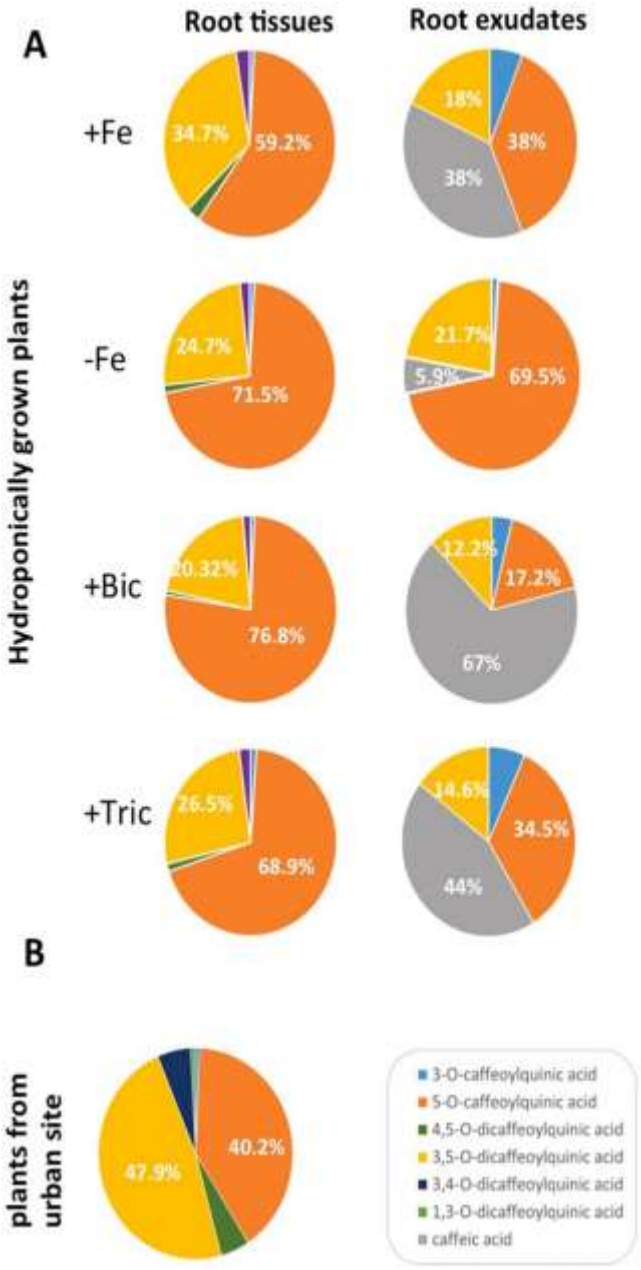

Fig. 8. Profile of caffeoylquinic acid derivatives identified in extracted fraction from tissues (left panel) and exudates fraction (right panel) of root of *P. judaica* grown hydroponically in +Fe, -Fe, Bic, and Tric treatments (A). Profile of caffeoylquinic acid derivatives identified in *P. judaica* harvested from the soil (urban soil) is reported in B. Percentage Pie chart is related to a representative experiment with three independent replicates (n = 3).

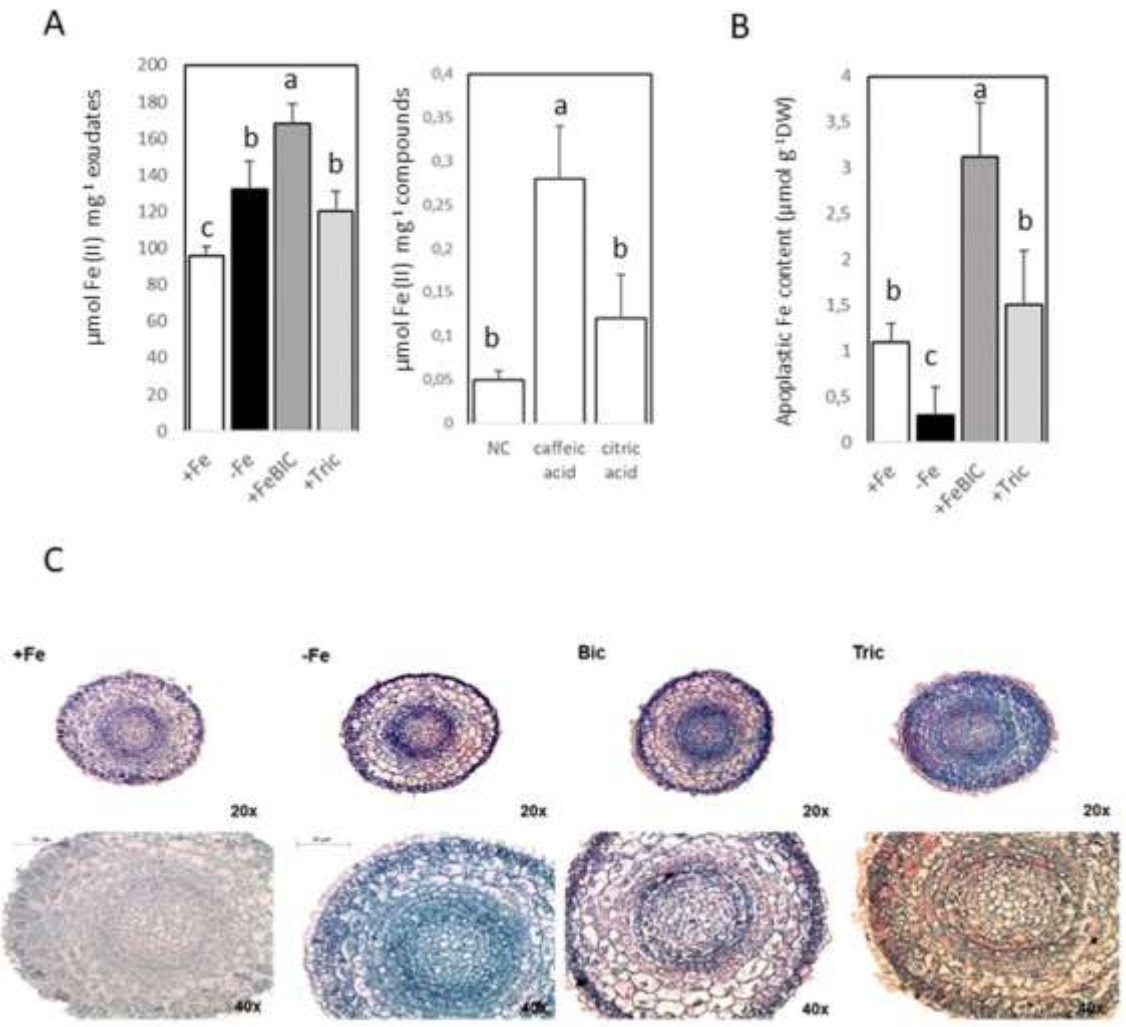

Fig. 9. A) Fe (III) reduction activity of root exudates, caffeic and citric acids; B) Fe content in the root apoplast fraction and C) lignin visualization (red color) in root cross sections of *P. judaica* grown in +Fe, -Fe, Bic, and Tric treatments (20x and 40x magnification). Different letters correspond to significant differences among means ($P < 0.05$; Tukey test), n = 3. (For interpretation of the references to color in this figure legend, the reader is referred to the Web version of this article.)

Table 1

Principal components of root traits of rooted cuttings of *Parietaria judaica* exposed to different treatments (+Fe, -Fe, Bic and Tric).

	Attribute loadings	
	PC1	PC2
Statistics		
Eigenvalue and variability		
Eigenvalue	2.474	1.919
Proportion of variability (%)	49	38
Variable		
Eigenvectors		
Tissue density (TD)	**-.867**	.071
Total length lateral roots (LI)	.192	**.959**
Average length adventitious roots (aLA)	**.926**	.073
Average length lateral roots (aLI)	-.074	**.981**
Root branching zone (BZ)	**.907**	.165

Table S1. Abbreviation of root parameters determined and mentioned in the text

parameters	Adventitious root	1st-order laterals roots	Whole roots
length	LA	LI	LT
number	NA	NI	-
average lenght	aLA	aLI	-
surface	SA	SI	ST
volume	VA	VI	VT
ary weight	WA	WI	WT

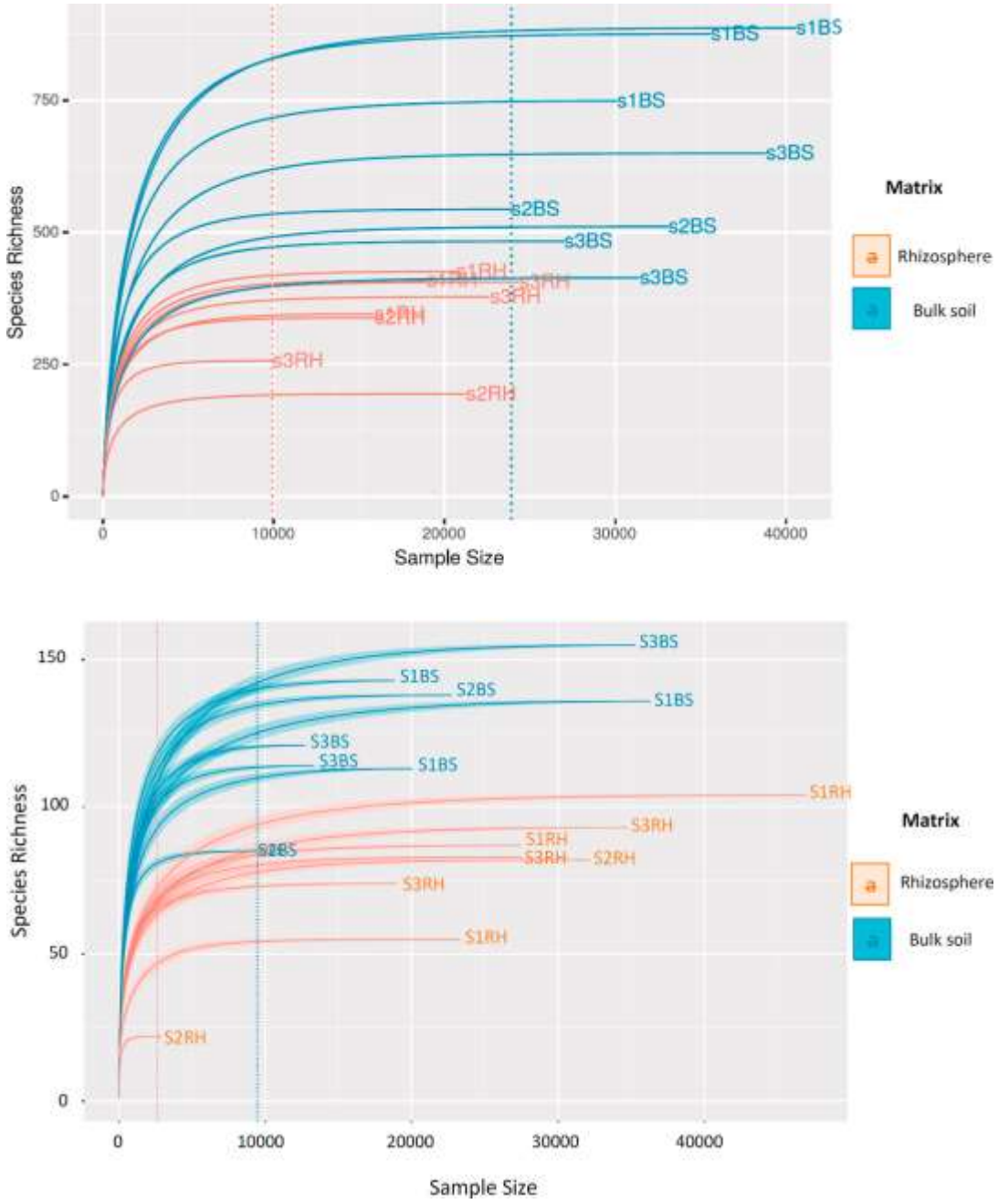

Fig. S1. Rarefaction curves showing the reaching of a satisfactory sequencing depth for each of the sequenced samples. Upper panel: prokaryotic libraries; lower panel: fungal libraries.

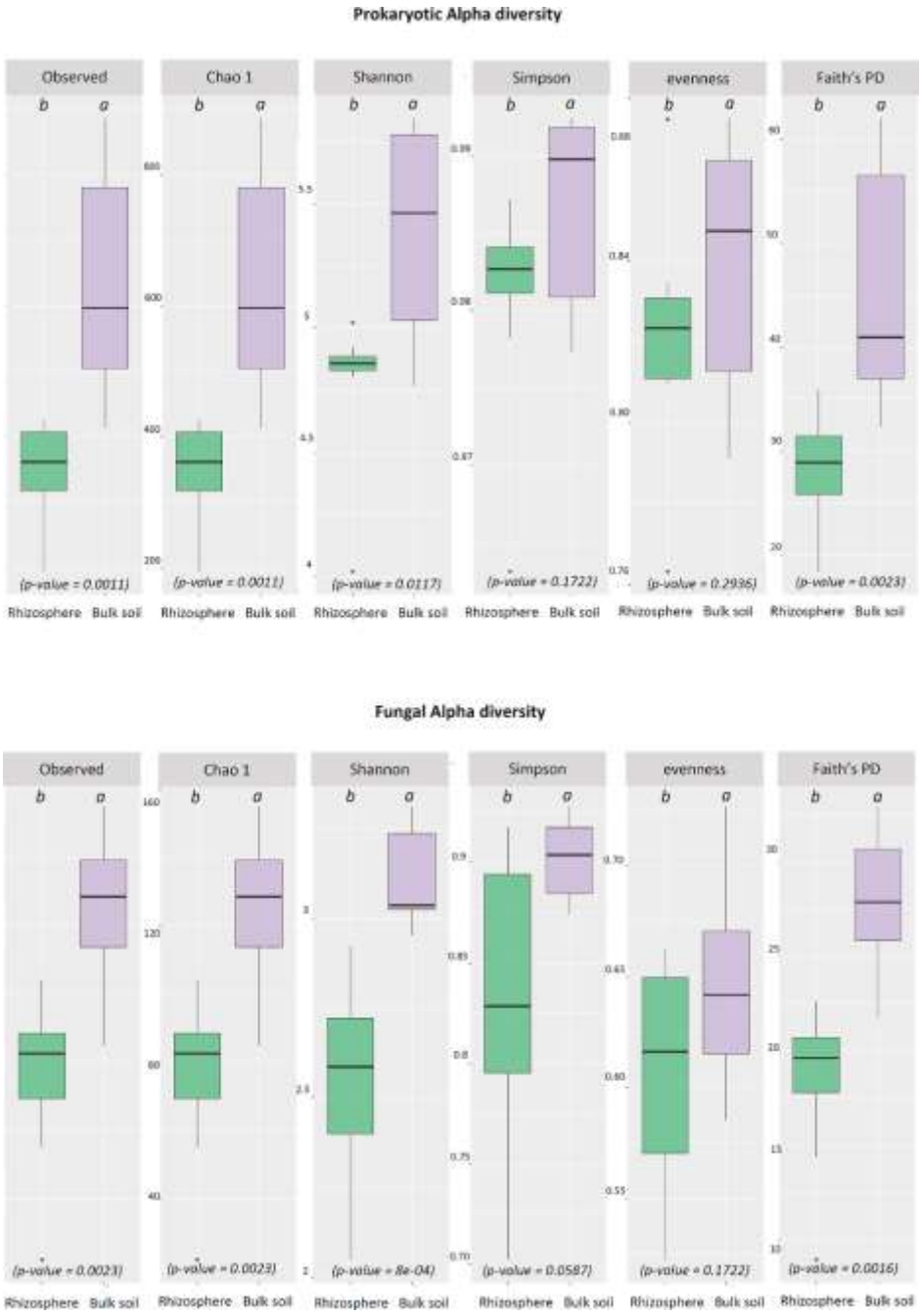

Fig. S2. Alpha indexes showing the OTUs diversities between rhizosphere and bulk soil.

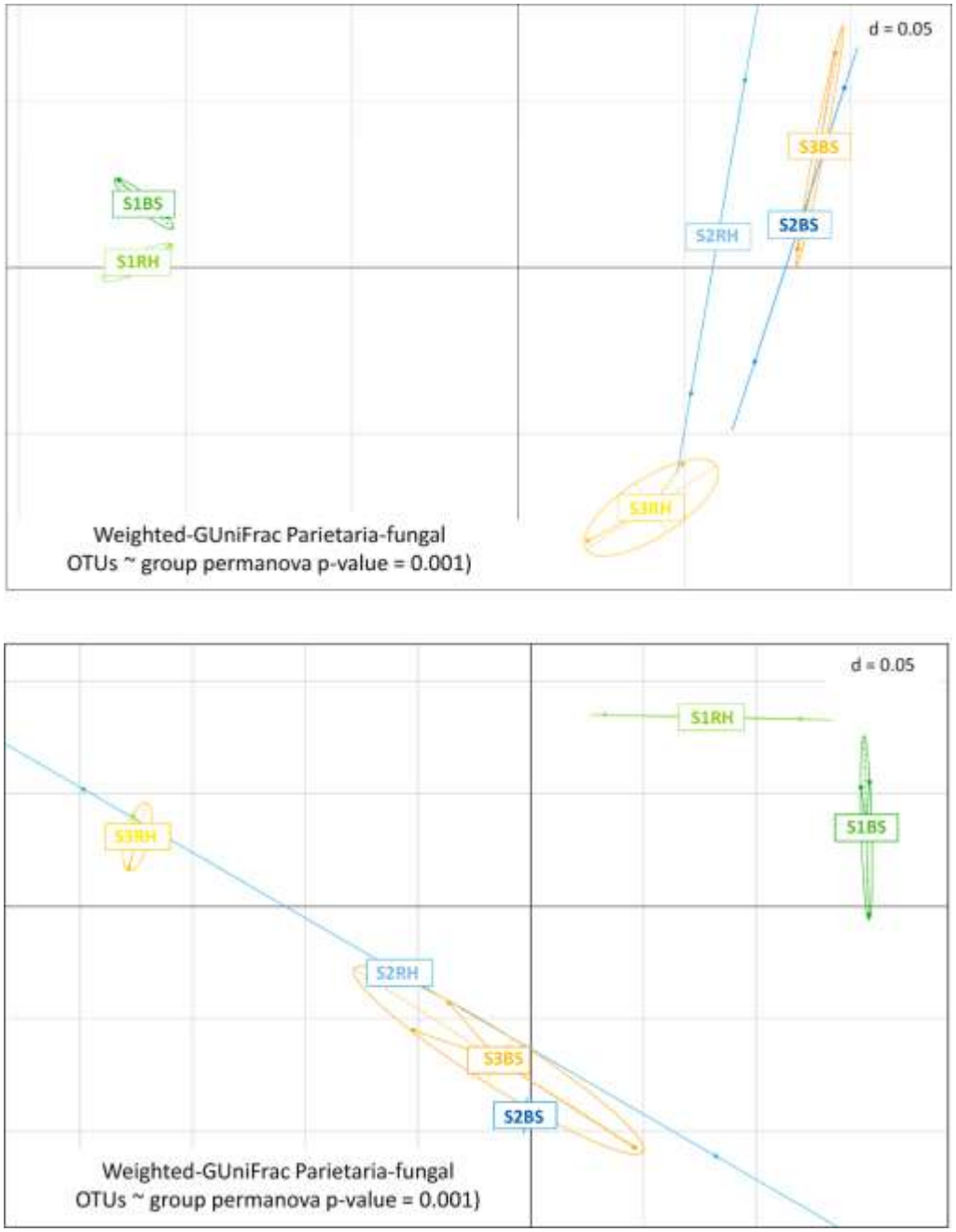

Fig. S3. Weighted Generalized Unifrac analysis showing the intra-groups diversity of the Prokaryotic (upper diagram) and Fungal (lower diagram) microbial communities between the two conditions considered (BS= Bulk soil; RH = Rhizosphere samples).

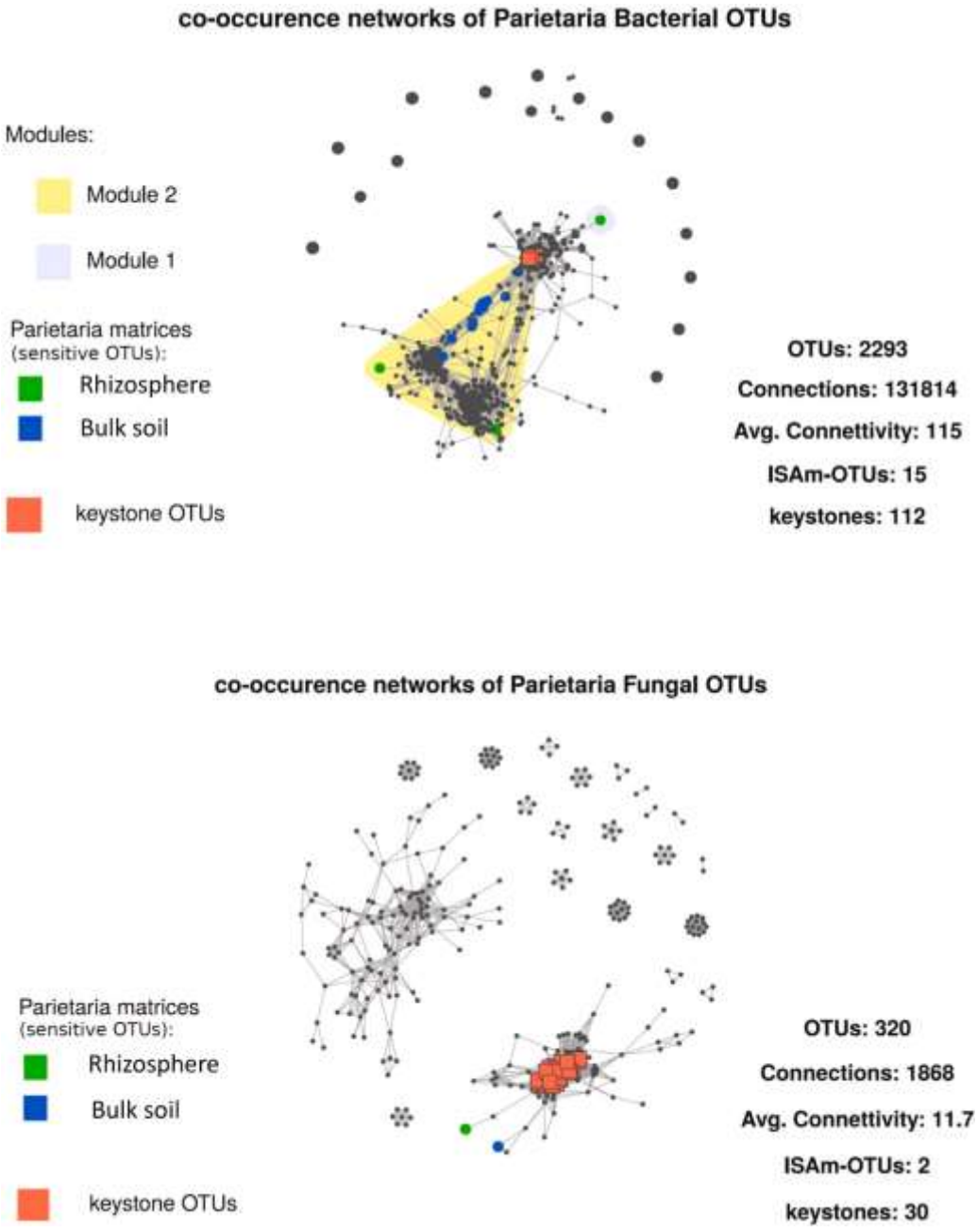

Fig. S4. Co-occurrence networks visualising the positive, significant correlations ($\rho > 0.7$ and $p < 0.001$) among prokaryotic (upper diagram) and fungal OTUs (lower diagram) from the Rhizosphere and the Bulk soil microbial communities. The sensitive OTUs shown in green and blue represent the OTUs identified as indicator species for the rhizosphere and bulk soil condition, respectively (listed in supplemental file 3). Red squares represent the keystone OTUs (listed in supplemental file 2). Modules are defined as areas that show a high density of connections among OTUs. The Gray symbols represent "hot spots" of overlapping OTUs.

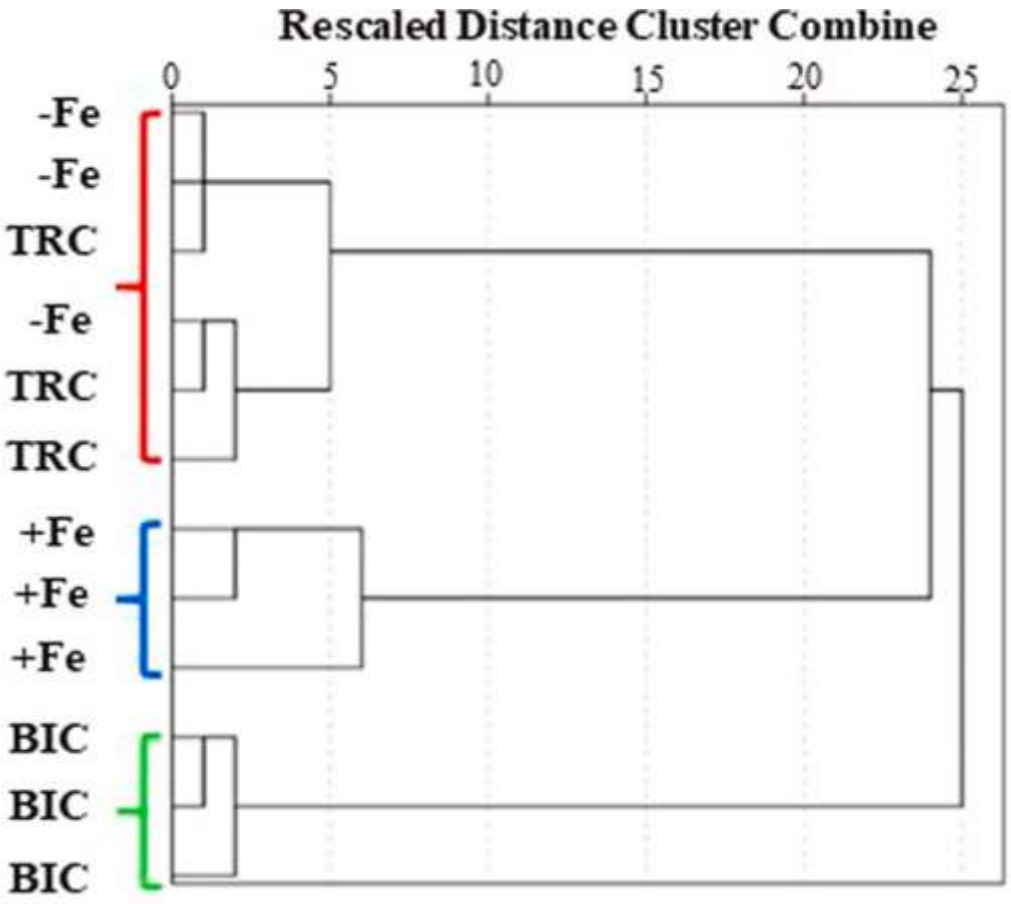

Fig. S5. Dendrogram of Hierarchical Cluster Analysis of the scores of the PCA using the Ward's method with distance measure by squared Euclidean distance.

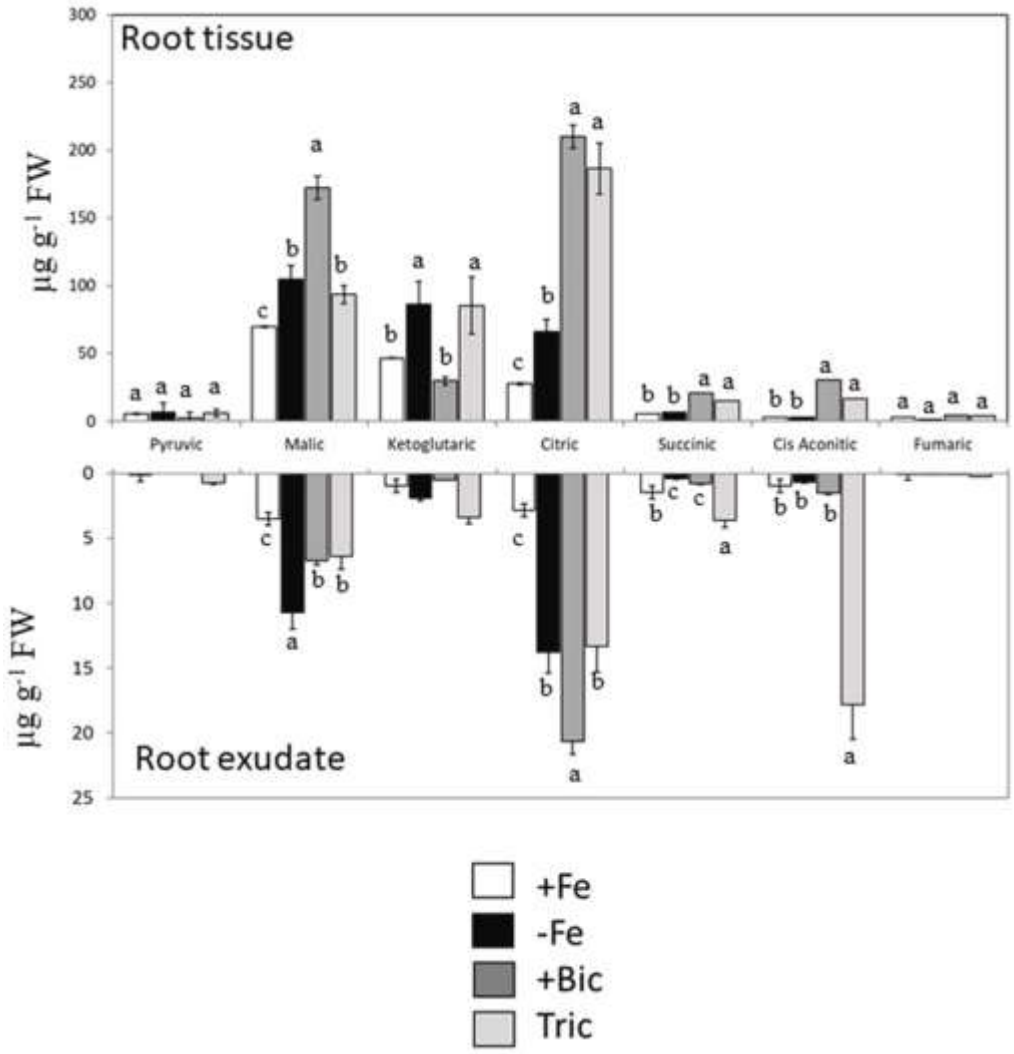

Fig. S6. Characterization of carboxylic acids concentrations in root tissues (upper panel) and root exudates (lower panel) of P. judaica grown in +Fe, -Fe, Bic, and Tric treatments. Different letters correspond to significant differences among mean values ($P < 0.05$; Tukey test), $n = 3$.

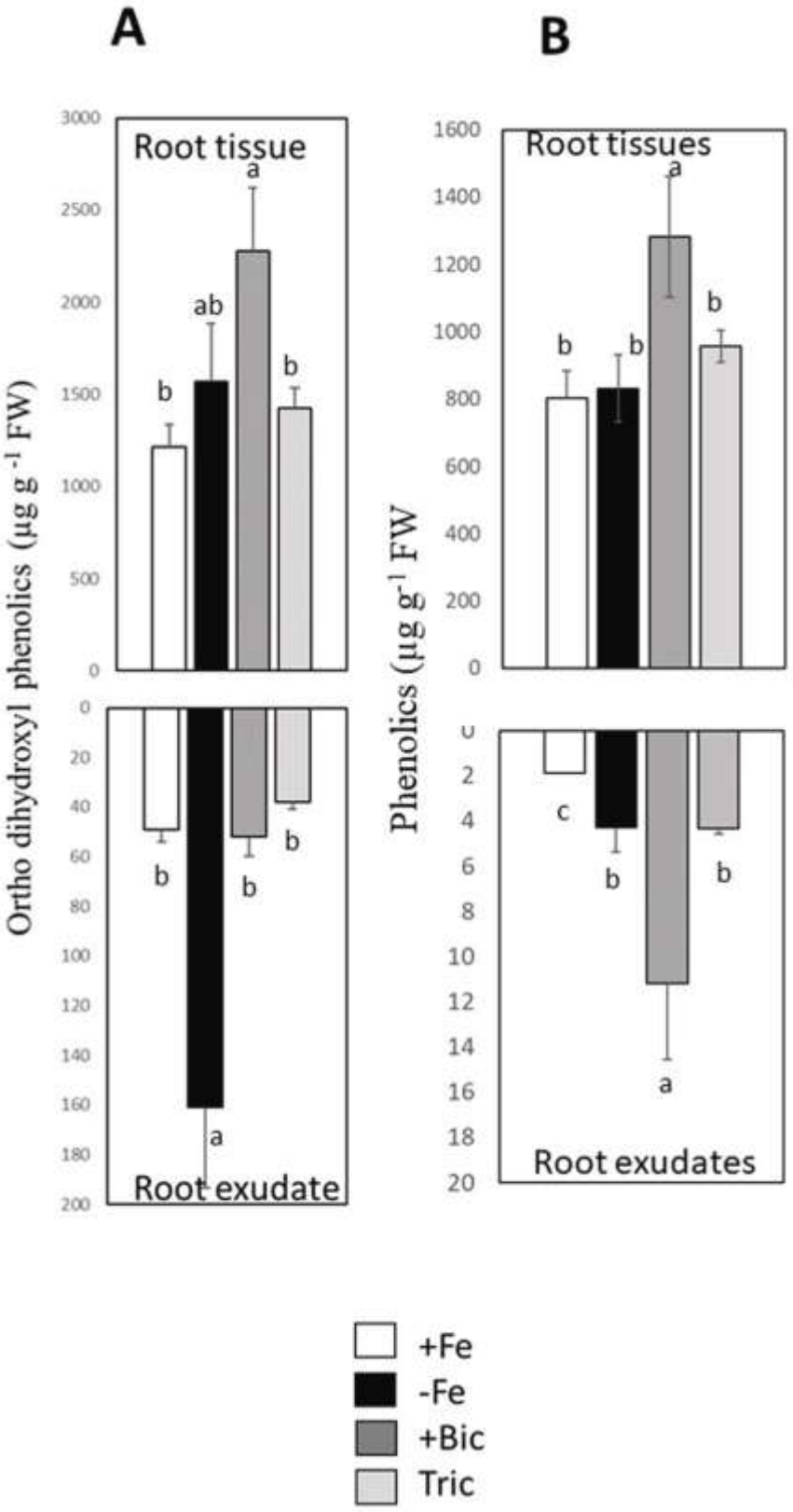

Fig. S7. Quantification of the phenolics compounds by Arnowns' reagent (A) and by HLPC-DAD (B) approaches. Different letters correspond to significant differences among means ($P < 0.05$; Tukey test), n = 3

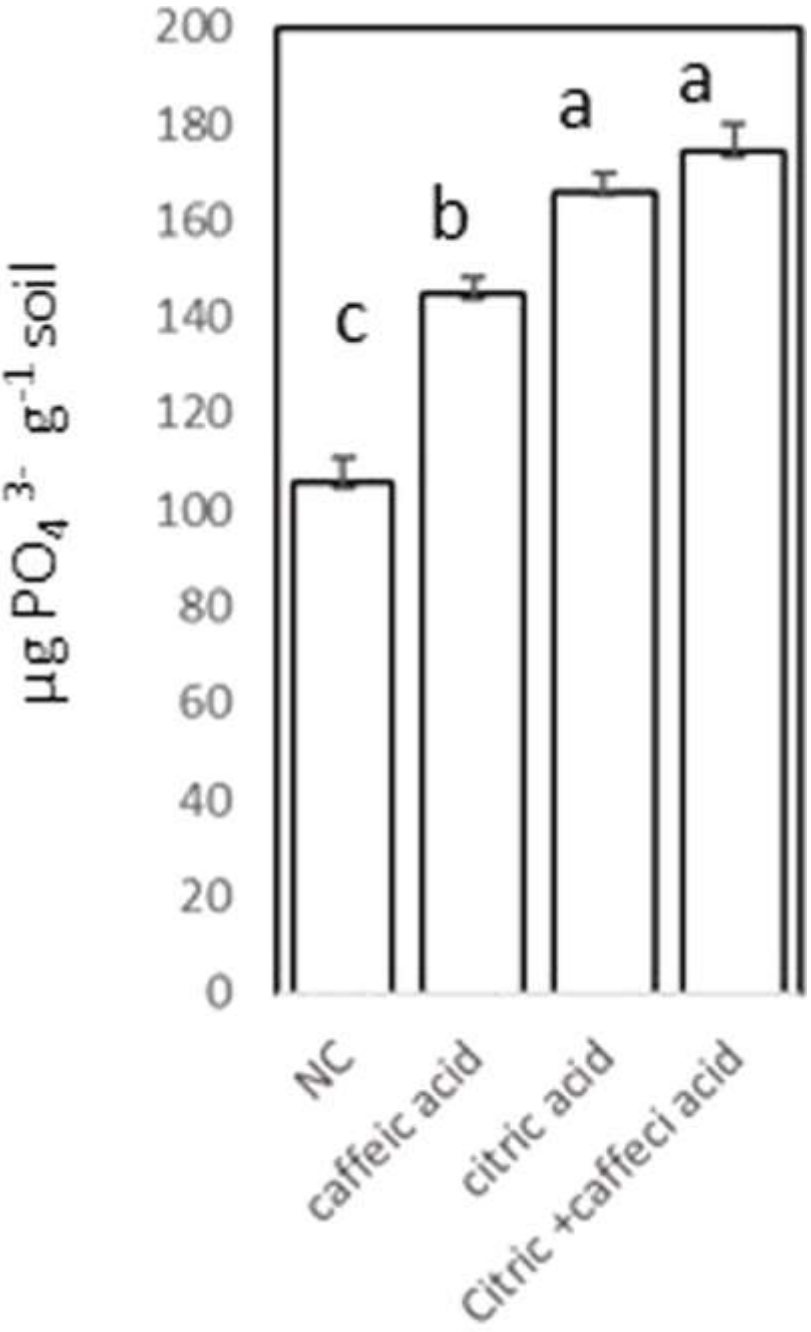

Fig. S8. Content of phosphate anions in soluble fraction of urban soils after incubation with caffeic and citric acids. Different letters correspond to significant differences among mean values ($P < 0.05$; Tukey test), $n = 3$.